AD-A040 594 ANALYTIC SCIENCES CORP READING MASS F/G 20/4
AN EXTENDED KALMAN FILTER FOR ESTIMATING AERODYNAMIC COEFFICIEN--ETC(U)
DEC 76 C M BROWN F08635-76-C-0117
UNCLASSIFIED TASC-TR-636-1 AFATL-TR-76-158 NL

1 OF 1
AD A040 594

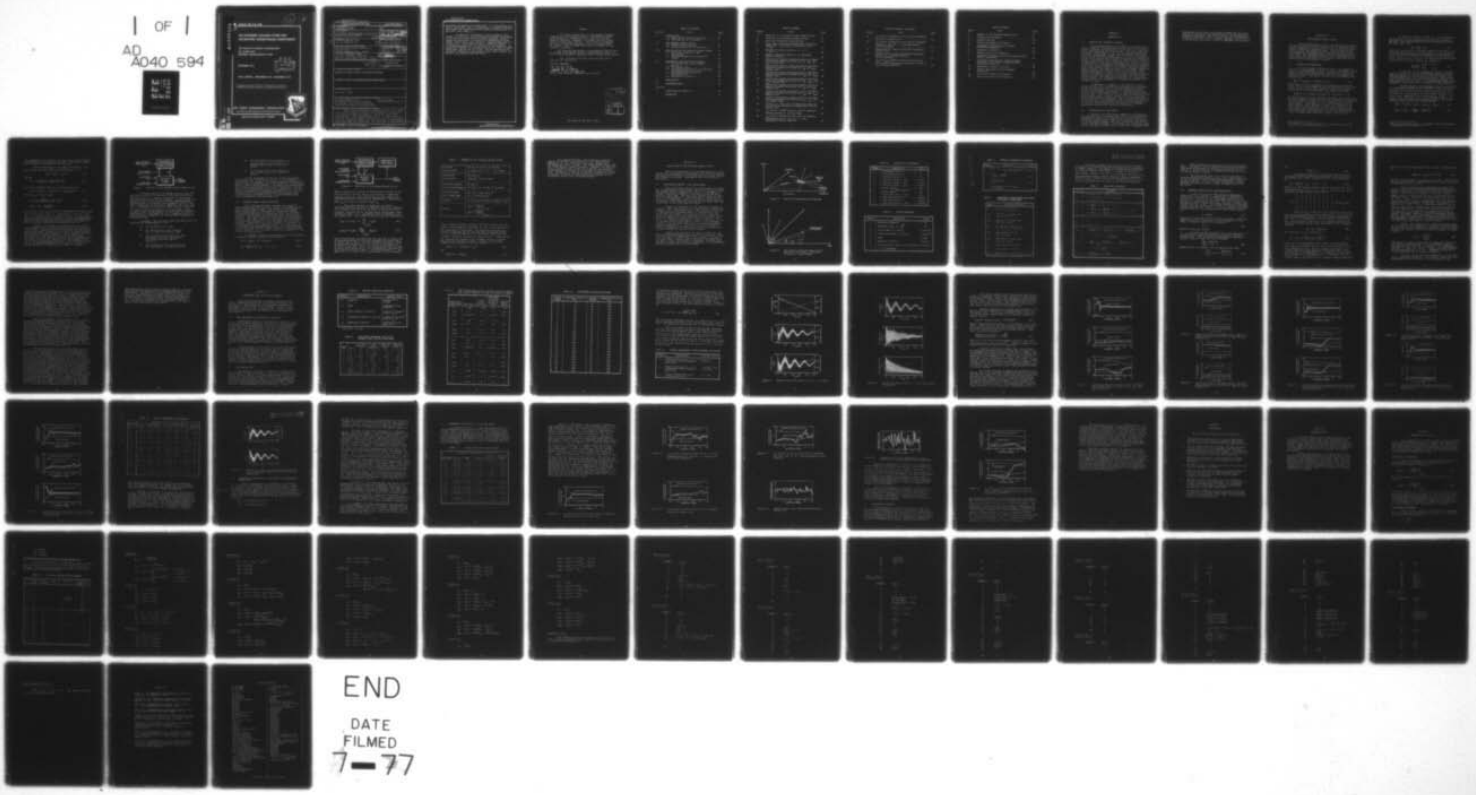

END

DATE FILMED
7-77

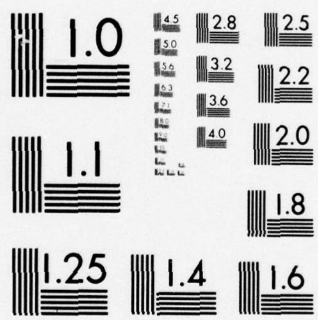

MICROCOPY RESOLUTION TEST CHART
NATIONAL BUREAU OF STANDARDS-1963-A

AFATL-TR-76-158

AN EXTENDED KALMAN FILTER FOR ESTIMATING AERODYNAMIC COEFFICIENTS

THE ANALYTIC SCIENCES CORPORATION
SIX JACOB WAY
READING, MASSACHUSETTS 01867

DECEMBER 1976

FINAL REPORT: SEPTEMBER 1975- SEPTEMBER 1976

APPROVED FOR PUBLIC RELEASE; DISTRIBUTION UNLIMITED.

AIR FORCE ARMAMENT LABORATORY
AIR FORCE SYSTEMS COMMAND • UNITED STATES AIR FORCE
EGLIN AIR FORCE BASE, FLORIDA

UNCLASSIFIED

SECURITY CLASSIFICATION OF THIS PAGE (When Data Entered)

REPORT DOCUMENTATION PAGE

READ INSTRUCTIONS BEFORE COMPLETING FORM

1. REPORT NUMBER: AFATL-TR-76-158
2. GOVT ACCESSION NO.
3. RECIPIENT'S CATALOG NUMBER

4. TITLE (and Subtitle): AN EXTENDED KALMAN FILTER FOR ESTIMATING AERODYNAMIC COEFFICIENTS

5. TYPE OF REPORT & PERIOD COVERED: Final Report. Sept 1975 - Sept 1976

6. PERFORMING ORG. REPORT NUMBER: TASC-TR-636-1

7. AUTHOR(s): Charles M. Brown, Jr

8. CONTRACT OR GRANT NUMBER(s): F08635-76-C-0117

9. PERFORMING ORGANIZATION NAME AND ADDRESS
The Analytic Sciences Corporation
Six Jacob Way
Reading, Massachusetts 01867

10. PROGRAM ELEMENT, PROJECT, TASK AREA & WORK UNIT NUMBERS
Project No. 2547
Task No. 04
Work Unit No. 012

11. CONTROLLING OFFICE NAME AND ADDRESS
Air Force Armament Laboratory
Armament Development and Test Center
Eglin Air Force Base, Florida 32542

12. REPORT DATE: Dec 1976

13. NUMBER OF PAGES: 70

14. MONITORING AGENCY NAME & ADDRESS (if different from Controlling Office): 69 p.

15. SECURITY CLASS. (of this report): UNCLASSIFIED

15a. DECLASSIFICATION/DOWNGRADING SCHEDULE

16. DISTRIBUTION STATEMENT (of this Report)

Approved for public release; distribution unlimited.

17. DISTRIBUTION STATEMENT (of the abstract entered in Block 20, if different from Report)

62602F

18. SUPPLEMENTARY NOTES

Available in DDC

19. KEY WORDS (Continue on reverse side if necessary and identify by block number)

Extended Kalman Filter
Aerodynamic Coefficient Estimates
Free-Flight Trajectory Measurements
Nonlinear Six-Degree-of-Freedom Model
EKF Algorithm
Dynamic Modeling Errors

20. ABSTRACT (Continue on reverse side if necessary and identify by block number)

This report describes an extended Kalman filter (EKF) algorithm developed to estimate the aerodynamic coefficients of projectiles, based on discrete free-flight trajectory measurements. These measurements consist of three spatial positions and three angular orientations, relative to a fixed inertial coordinate system, and time-of-flight at 50 downrange positions along the trajectory. The algorithm is based upon a

→ next page

DD FORM 1 JAN 73 1473 EDITION OF 1 NOV 65 IS OBSOLETE

UNCLASSIFIED

SECURITY CLASSIFICATION OF THIS PAGE (When Data Entered)

nonlinear six-degree-of-freedom model of a rotationally symmetric rigid body, and it incorporates a stochastic measurement model that approximates the conditions which exist in a ballistic test range.

In addition to estimates of the projectile aerodynamic coefficients, the EKF algorithm provides an estimate of the rms error associated with each parameter estimate. Algorithm performance is evaluated by estimating the aerodynamic coefficients from synthetic, computer-generated trajectory data. This report presents evaluation results including assessments of the accuracy of the estimates; the consistency between the estimation errors and their standard deviations computed by the filter; and the sensitivity to projectile trajectory, measurement noise level, initial conditions, and dynamic modeling errors.

PREFACE

This report was prepared by The Analytic Sciences Corporation, Six Jacob Way, Reading, Massachusetts 01867 under Contract No. F08635-76-C-0117 with the Air Force Armament Laboratory, Armament Development and Test Center, Eglin Air Force Base, Florida. This effort was conducted during the period from September 1975 to September 1976. Dr. Donald C. Daniel (DLDL) monitored the program for the Armament Laboratory.

This report has been reviewed by the Information Office (OI) and is releasable to the National Technical Information Service (NTIS). At NTIS, it will be available to the general public, including foreign nations.

This technical report has been reviewed and is approved for publication.

FOR THE COMMANDER:

Gerald P. D'Arcy

GERALD P. D'ARCY, Colonel, USAF
Chief, Guns, Rockets, and Explosives Division

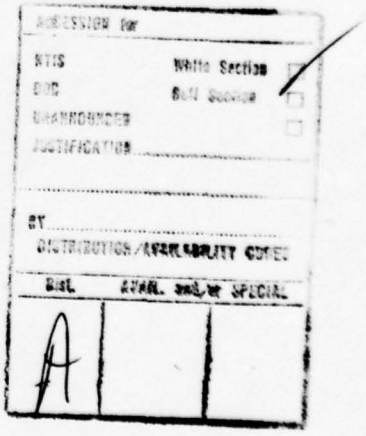

(The reverse of this page is blank)

TABLE OF CONTENTS

LIST OF FIGURES

LIST OF FIGURES (Concluded)

LIST OF TABLES

SECTION I

INTRODUCTION

1.1 OVERVIEW AND TECHNICAL APPROACH

The extended Kalman filter (EKF) is a general nonlinear estimation technique which can be applied to the problem of estimating the aerodynamic coefficients of a body from free-flight measurements of its motion. The basic technique can handle a wide range of nonlinear aerodynamic models and trajectory measurement systems, and it accounts for random errors in the trajectory measurements, stochastic disturbances to the body's motion, and a priori information about the aerodynamic coefficients to be estimated. This report describes an application of the EKF to the estimation of the aerodynamic coefficients of a six-degree-of-freedom rotationally symmetric rigid body, based on discrete free-flight trajectory measurements, such as those made at the Air Force Armament Laboratory (AFATL) Aeroballistic Research Facility test range. These measurements consist of three spatial positions and three angular orientations, relative to a fixed inertial coordinate system, and time-of-flight at 50 downrange positions along the trajectory. The algorithm incorporates a stochastic measurement model that approximates the conditions which exist at the test range.

In addition to estimates of the projectile aerodynamic coefficients, the EKF algorithm provides an estimate of the rms error associated with each parameter estimate. Algorithm performance is evaluated by estimating the aerodynamic coefficients from synthetic, computer-generated trajectory data. These data are derived from the same projectile dynamic model that is used to design the filter algorithm. This report presents evaluation results including assessments of the accuracy of the estimates; the consistency between the estimation errors and their standard deviations computed by the filter; and the sensitivity to projectile trajectory, measurement noise level, and initial conditions.

1.2 ORGANIZATION OF THE REPORT

Section II of this report summarizes and discusses the equations of the extended Kalman filter and provides the mathematical basis for its application to the estimation of aerodynamic coefficients. Section III describes the details of the projectile dynamic model and illustrates the application of the EKF technique. Performance and sensitivity study results are given in Section IV, and Section V summarizes the

conclusions of the study and provides suggestions for future related investigations and applications of the EKF parameter estimation technique. Section VI presents the recommendations resulting from this effort. Finally, Appendix A gives some of the detailed equations required to implement the algorithm.

SECTION II

THE EXTENDED KALMAN FILTER

The extended Kalman filter is an extension of optimal (minimum-variance) linear filtering theory to problems which involve significant nonlinearities, e.g., the projectile aerodynamic coefficient estimation task. This section provides the background, mathematical models, and notational conventions needed for understanding the EKF algorithm developed in this study. The discussion assumes a basic familiarity with random variables and state-space notation; additional details can be found in References 1 through 8.

2.1 KALMAN FILTER EQUATIONS

To apply Kalman filtering theory to any estimation problem, it is necessary to derive a linear, stochastic, first-order, vector matrix differential equation which models the manner in which the system states interact and propagate as a function of time. For linear systems, this equation has the general form

$$\dot{\underline{x}}(t) = F(t)\underline{x}(t) + G(t)\underline{w}(t) + \underline{u}(t) \qquad (1)$$

where $\underline{x}(t)$ is an $n\times 1$ column vector representing the system state, $F(t)$ is an $n\times n$ dynamics matrix which defines the interaction of the state vector components, and $\underline{w}(t)$ is a $p\times 1$ column vector of white gaussian noise inputs such that*

$$E[\underline{w}(t)] = \underline{0};\ \mathrm{Cov}[\underline{w}] = E[\underline{w}(t)\underline{w}(\tau)^T] = Q(t)\delta(t-\tau) \qquad (2)$$

The matrix $G(t)$ is an $n\times p$ distribution matrix which indicates how each component of $\underline{w}(t)$ affects each component of the system state derivative, and $\underline{u}(t)$ is a $n\times 1$ column vector of known system inputs. Note that the F, G, and Q matrices may be time-varying. For a projectile model, the elements of the state vector $\underline{x}$ will typically be projectile positions and velocities, the elements of $\underline{w}$ will be random inputs such as wind disturbances and turbulence effects, and the elements of $\underline{u}$ will be known inputs such as average wind velocity.

---

*The symbol E[ ] denotes mathematical expectation; Cov [$\underline{w}$] denotes the covariance matrix of $\underline{w}$.

At discrete instants of time, t_k, it is assumed that measurements of linear combinations of the state variables are made. The equation describing this measurement process has the general form

$$\underline{z}_k = H_k \underline{x}_k + \underline{v}_k \tag{3}$$

where $\underline{z}_k$ is a vector of r measured quantities at time t_k, H_k is an r×n observation matrix describing the linear combinations of state variables which comprise $\underline{z}_k$ in the absence of noise, and $\underline{v}_k$ is an r vector of zero mean gaussian measurement errors with a covariance matrix, R_k, defined by

$$E\left[\underline{v}_k \underline{v}_j^T\right] = \begin{cases} [0] & ; \quad k \neq j \\ R_k & ; \quad k = j \end{cases} \tag{4}$$

At any time t, the objective of optimal estimation theory is to process all the measurements taken up to that time and produce an estimate $\hat{\underline{x}}(t)$ of the system state $\underline{x}(t)$ having minimum error, in a statistical sense. The optimization criterion most often chosen is that of minimizing the mean square estimation error. This minimum mean-square error estimate is calculated with the Kalman filtering algorithm.

As measurements become available, there is essentially an instantaneous change in the knowledge of the state $\underline{x}(t_k)$. Denoting the optimum estimate of $\underline{x}(t_k)$ just prior to the availability of $\underline{z}_k$ as $\hat{\underline{x}}_k(-)$ and the optimum estimate of the state vector immediately after processing $\underline{z}_k$ as $\hat{\underline{x}}_k(+)$, the Kalman filter generates the optimum estimate of the system state according to the following algorithm:*

$$\dot{\hat{\underline{x}}}(t) = F(t)\hat{\underline{x}}(t) + \underline{u}(t) \; ; \; \hat{\underline{x}}(t_{k-1}) = \hat{\underline{x}}_{k-1}(+) \tag{5}$$

$$\hat{\underline{x}}_k(+) = \hat{\underline{x}}_k(-) + K_k\left[\underline{z}_k - H_k \hat{\underline{x}}_k(-)\right] \tag{6}$$

---

*Only the continuous form of the Kalman filter with discrete measurements is considered here.

where Equation (5) is used to calculate the estimate between measurements and Equation (6) is used to update the estimate when new data is received at each time t_k.

The n×r matrix K_k is the Kalman gain matrix. Let $\underline{\tilde{x}}(t)$ denote the error made in estimating $\underline{x}(t)$, i.e.,

$$\underline{\tilde{x}}(t) = \underline{\hat{x}}(t) - \underline{x}(t) \tag{7}$$

and let

$$P(t) = \mathrm{Cov}\left[\underline{\tilde{x}}(t)\right] = E\left[\underline{\tilde{x}}(t)\underline{\tilde{x}}(t)^T\right] \tag{8}$$

K_k is then computed using the following equations:

$$\dot{P}(t) = F(t)P(t) + P(t)F(t)^T + G(t)Q(t)G(t)^T \tag{9}$$

with $P(t_{k-1}) = P_{k-1}(+)$ and

$$K_k = P_k(-)H_k^T\left[H_kP_k(-)H_k^T + R_k\right]^{-1} \tag{10}$$

$$P_k(+) = \left[I - K_kH_k\right]P_k(-) \tag{11}$$

where $P_k(-)$ is P(t) just before the measurement at time t_k and $P_k(+)$ is P(t) just after t_k. Equation (9) is used to calculate the estimation error covariance between the measurements; Equations (10) and (11) are used to calculate the Kalman gain matrix for use in Equation (6) and to update the estimation error covariance matrix when a measurement arrives.

Figure 1 illustrates the structure of the optimal linear Kalman filter. This estimation algorithm has two distinct phases. Equations (5) and (9) describe the time evolution of the state estimate and its error statistics between measurements under the influence of system dynamics and noise. This process is commonly referred to as extrapolation. Equations (6), (10), and (11) indicate how the estimate and its error covariance are updated at the measurement time to reflect the new information available. The algorithm is optimum in the minimum mean-square error sense as long as the assumed mathematical model for the system is accurate.

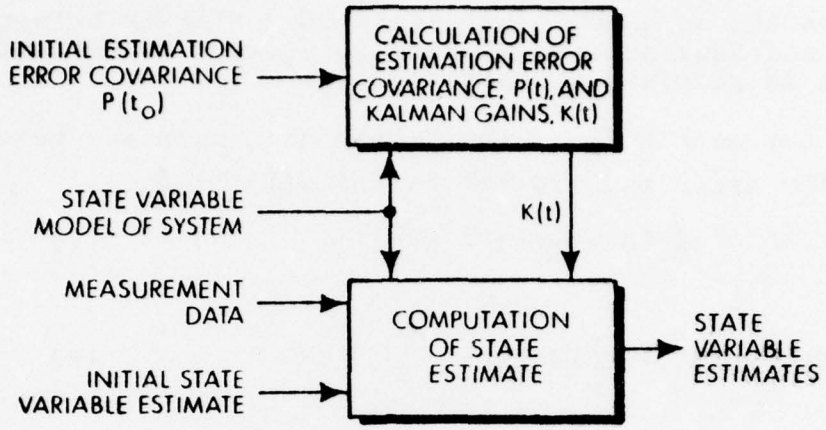

Figure 1. Structure of an Optimal Linear Kalman Filter

A unique feature of the Kalman filter is that the performance analysis is inherent in the algorithm for K_k. The matrix P(t) is a complete description of the second-order error statistics of the estimate. In particular, the diagonal terms of P(t) represent the minimum mean-square error obtained in estimating each component of $\underline{x}(t)$. Note P(t) is specified for all time by Equations (9), (10), and (11). Knowledge of neither $\underline{x}(t)$, $\hat{\underline{x}}(t)$, nor $\underline{z}_k$ is required to obtain a performance analysis for the optimal filter. In other words, the performance of the filter is completely determined by its mathematical model, assuming that this model accurately represents the system which generates the measurement data.

In summary, the following conditions must be met to implement an optimum Kalman filter:

- The system must be linear.
- The matrices F(t), G(t), and $\underline{u}(t)$ must be known functions of time.
- The vector input $\underline{w}(t)$ must be a zero mean gaussian white noise process with known covariance matrix, $Q(t)\delta(t-\tau)$.
- The measurements must obey Equation (3), and H_k must be known for all k.

- The measurement errors $\underline{v}_k$ must be a gaussian white sequence with its covariance matrix, R_k, and its mean known.

- To initialize the filter equations, the initial statistics of $\underline{x}$ must be known.

If the aerodynamic coefficient estimation problem could be put into a form which met all of the conditions listed above, the design of an optimal estimator would involve only the direct implementation of the Kalman filter equations. However, the projectile dynamics considered here are nonlinear; the linearity requirement is violated. Furthermore, the objective of estimating the projectile aerodynamic coefficients, which is tantamount to estimating parameters of the matrix F in Equation (1), introduces additional nonlinearity. One means of overcoming these problems is the extended Kalman filter described in the next subsection.

2.2 EXTENDED KALMAN FILTER EQUATIONS

Since the problem under consideration cannot be realistically modeled as a linear system, a nonlinear estimation technique must be used. One method is the extended Kalman filter which is essentially a conventional Kalman filter design applied to a mathematical model of the system obtained by linearizing the system about the current state estimate. The structure of this algorithm is illustrated in Figure 2. Note that, because of the linearization procedure, the covariance calculation is now dependent upon the state estimate. Consequently, it is not possible to calculate the covariance matrix, as a function of time, off-line since it is dependent upon the measurement data. The extended Kalman filter yields very nearly optimal estimates if the linearization is accurate, i.e., as long as the state estimate is close to the true system state.

A reasonably general mathematical model for nonlinear stochastic systems is given by the equations

$$\dot{\underline{x}}(t) = \underline{f}[\underline{x}(t),\ t] + G(t)\underline{w}(t) \tag{12}$$

$$\underline{z}_k = \underline{h}_k\left[\underline{x}(t_k)\right] + \underline{v}_k \ ; \quad k = 1,2,\ldots \tag{13}$$

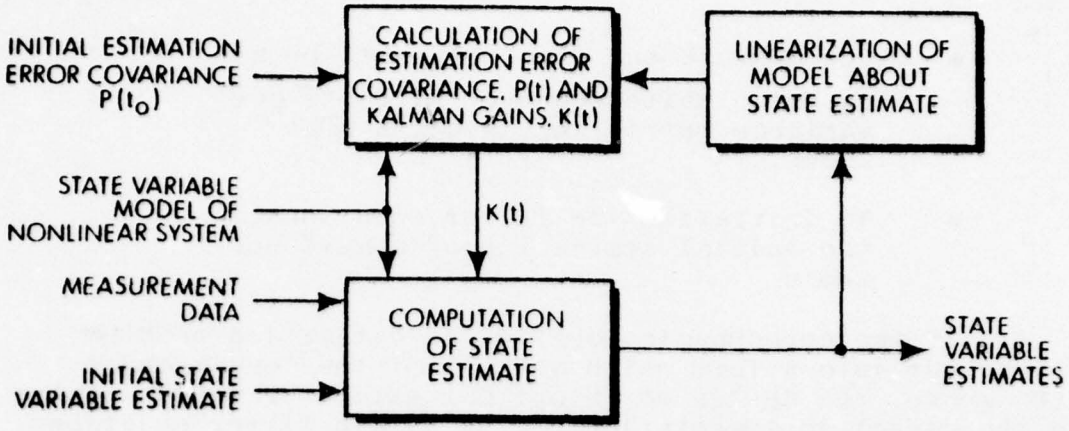

Figure 2. Structure of an Extended Kalman Filter

where $\underline{f}$ and $\underline{h}_k$ are nonlinear differentiable functions of the state vector $\underline{x}$, and $\underline{w}(t)$ and $\underline{v}_k$ are zero mean, independent gaussian white noise processes having spectral density and covariance matrices, $Q(t)$ and R_k, respectively. The measurements $\underline{z}_k$ are taken at discrete times t_k.

The first approach one might use to derive a filtering algorithm for $\underline{x}(t)$ in Equation (12) is to linearize the nonlinear functions $\underline{f}$ and $\underline{h}_k$ about an appropriate known reference trajectory $\bar{\underline{x}}(t)$, and then apply conventional linear estimation theory, i.e., the Kalman filter discussed in the last subsection. Thus, denoting $\underline{x}(t_k)$ by $\underline{x}_k$, the expressions

$$\underline{f}(\underline{x},\ t) \cong \underline{f}(\underline{x},\ t) + \left.\frac{\partial \underline{f}}{\partial \underline{x}}\right|_{\underline{x}=\bar{\underline{x}}} (\underline{x}-\bar{\underline{x}}) \tag{14}$$

$$\underline{h}_k(\underline{x}_k) \cong \underline{h}_k(\bar{\underline{x}}_k) + \left.\frac{\partial \underline{h}_k}{\partial \underline{x}_k}\right|_{\underline{x}_k=\bar{\underline{x}}} (\underline{x}_k-\bar{\underline{x}}_k) \tag{15}$$

may be substituted into Equations (12) and (13) to derive the corresponding Kalman filter which estimates the variation in $\underline{x}$, $\delta\underline{x}(t) = \underline{x}(t) - \bar{\underline{x}}(t)$, from the reference trajectory. When the reference trajectory is chosen to be the current best estimate of the state, $\hat{\underline{x}}(t)$, the resulting algorithm is known as an extended Kalman filter; the mechanization equations for the latter are given in Table 1 (see also Reference 1). The matrix $P(t)$ is a first-order approximation to the estimation

TABLE 1. SUMMARY OF THE EXTENDED KALMAN FILTER

System Model	$\dot{\underline{x}}(t) = \underline{f}[\underline{x}(t),\ t] + G(t)\underline{w}(t)\ ;\ \underline{w}(t) \sim N[0,\ Q(t)]$
Measurement Model	$\underline{z}_k = \underline{h}_k[\underline{x}(t_k)] + \underline{v}_k\ ;\ k = 1, 2, \ldots\ ;\ \underline{v}_k \sim N(0,\ R_k)$
Initial Conditions	$\underline{x}(0) \sim N(\hat{\underline{x}}_o,\ P_o)$
Other Assumptions	$E\left[\underline{w}(t)\underline{v}_k^T\right] = 0$ for all k and all t
State Estimate Propagation	$\dot{\hat{\underline{x}}}(t) = \underline{f}[\hat{\underline{x}}(t),\ t]$
Error Covariance Propagation	$\dot{P}(t) = F[\hat{\underline{x}}(t),\ t]P(t) + P(t)F[\hat{\underline{x}}(t),\ t]^T + G(t)Q(t)G(t)^T$
State Estimate Update	$\hat{\underline{x}}_k(t) = \hat{\underline{x}}_k(-) + K_k\left\{\underline{z}_k - \underline{h}_k[\hat{\underline{x}}_k(-)]\right\}$
Error Covariance Update	$P_k(+) = \left\{I - K_k H_k[\hat{\underline{x}}_k(-)]\right\} P_k(-)$
Gain Matrix	$K_k = P_k(-)H_k[\hat{\underline{x}}_k(-)]^T \left\{H_k[\hat{\underline{x}}_k(-)]P_k(-)H_k[\hat{\underline{x}}_k(-)]^T + R_k\right\}^{-1}$
Definitions	$F[\hat{\underline{x}}(t),\ t] = \left.\dfrac{\partial \underline{f}[\underline{x}(t),\ t]}{\partial \underline{x}(t)}\right\|_{\underline{x}(t) = \hat{\underline{x}}(t)}$ $H_k[\hat{\underline{x}}(-)] = \left.\dfrac{\partial \underline{h}_k[\underline{x}(t_k)]}{\partial \underline{x}(t_k)}\right\|_{\underline{x}(t_k) = \hat{\underline{x}}(-)}$

error covariance matrix, and $\hat{\underline{x}}_k(-)$ and $P_k(-)$ denote the solutions to the propagation equations at time t_k just before the k^{th} measurement is processed. The principal practical difference in mechanizing the extended and conventional Kalman filters is that the gains K_k for the former depend upon the estimate; therefore, K_k must be computed online. Consequently, the computational burden of the extended filter is greater. Note that the equations in Table 1 reduce to the optimal Kalman filter outlined in the last section if

$$\underline{f}(\underline{x}(t),\ t) = F(t)\underline{x}(t) + \underline{u}(t) \tag{16}$$

and

$$\underline{h}_k(\underline{x}(t_k)) = H_k\underline{x}(t_k) \tag{17}$$

As a practical matter, one of the most important aspects of the EKF is the accuracy of the linearization (Equations (14) and (15)) about the state estimate $\hat{\underline{x}}(t)$. If the estimation error is large, this linearization is poor and the filter may not operate correctly. However, for the application considered here it has been found that the assumed linearization is satisfactory if the EKF is properly initialized. The details of the initialization procedure are given in Section III where the EKF equations are applied to the aerodynamic coefficient estimation problem.

SECTION III

APPLICATION OF THE EXTENDED KALMAN FILTER

This section describes how the EKF equations in subsection 2.2 are applied to aerodynamic coefficient estimation. The equations of motion of the system model are given, and an EKF design is developed. Performance results are given in Section IV.

3.1 EQUATIONS OF MOTION - THE SYSTEM MODEL

This subsection presents the system model upon which the extended Kalman filter design used in this study is based. The problem under consideration is that of a six-degree-of-freedom rotationally symmetric rigid body flying through a ballistic test range. The projectile dynamic model is taken directly from Reference 7. The equations of motion are derived in a fixed-plane coordinate system and assume that the aerodynamic coefficients are expanded as polynomial functions of the sine of the total angle-of-attack.

Figure 3 illustrates the two coordinate systems of interest. The first (x,y,z) is a fixed inertial system which assumes a flat, nonrotating earth. The second (x',y',z') is a fixed-plane axis system attached to the projectile but having zero roll angle. In this system, the x' axis lies along the projectile axis of symmetry, and the origin of the system is fixed to the projectile center-of-gravity. The (x',y',z') system is obtained by rotation of the (x,y,z) system through the two Euler angles ψ and θ in the indicated sequence. The projectile roll angle is measured clockwise looking downrange, i.e., from the tail of the projectile. Figure 4 illustrates the Euler angle rotations and the relationship between the two coordinate systems.

Twelve state variables are used to define the six-degree-of-freedom dynamic equations of the projectile. These state variables are summarized in Table 2 with their definitions and units. Table 3 defines the constants required by the model, Table 4 defines the intermediate variables used, and Table 5 gives the polynomial expansions of the aerodynamic coefficients which are to be estimated.

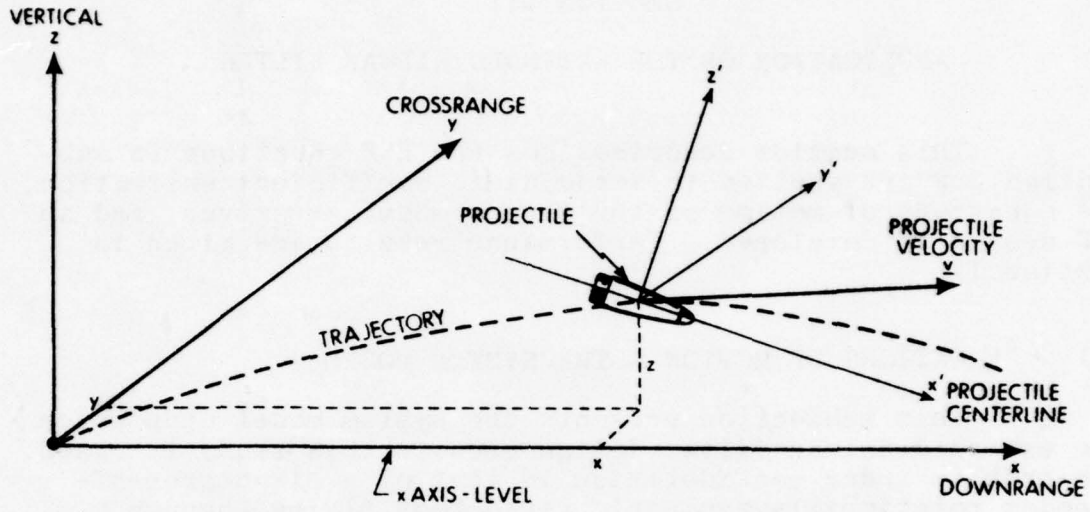

Figure 3. Earth and Fixed-Plane Axes Systems

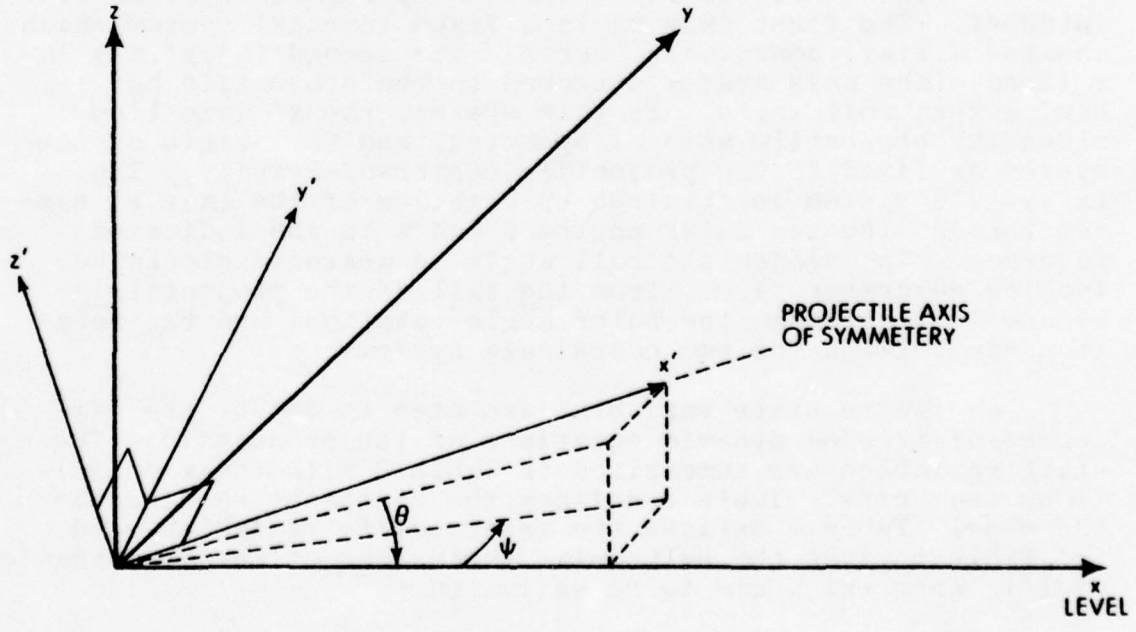

Figure 4. Euler Angle Rotations between Earth and Fixed Plane Axes - Directions of Positive ψ and θ Shown

TABLE 2. SYSTEM STATE VARIABLES

SYMBOL	DEFINITION	UNITS
x	Downrange position	ft
y	Crossrange position	ft
z	Vertical position	ft
u	Velocity along x' axis	ft/sec
v	Velocity along y' axis	ft/sec
w	Velocity along z' axis	ft/sec
ψ	Euler angle } See Figure 4	rad
θ	Euler angle } See Figure 4	rad
ϕ	Roll angle about x axis	rad
$\dot{\psi}$	Time derivative of ψ	rad/sec
$\dot{\theta}$	Time derivative of θ	rad/sec
p	Spin rate about x' axis	rad/sec

TABLE 3. SYSTEM CONSTANTS

SYMBOL	DEFINITION	UNITS
d	Reference diameter	ft
A	Reference area; $A = \frac{\pi d^2}{4}$	ft^2
I_x	Axial moment of inertia	$slug\text{-}ft^2$
I_y	Transverse moment of inertia	$slug\text{-}ft^2$
m	Mass	slugs
V_o	Reference velocity	ft/sec
g	Acceleration of gravity, g=32.17405	ft/sec^2
π	π = 3.1415926536	—

TABLE 4. SYSTEM INTERMEDIATE VARIABLES

SYMBOL	DEFINITION	UNITS
ρ	Air density; $\rho = 2.37692\text{x}10^{-3}\left[1-(6.8754\text{x}10^{-6})z\right]^{4.2561}$	$lb\text{-}sec^2/ft^4$
V	Velocity Magnitude: $V = \sqrt{u^2 + v^2 + w^2}$	ft/sec
$\bar{q}$	Dynamic pressure; $\bar{q} = 1/2\ \rho V^2$	lb/ft^2
ε	Sine of the total angle-of-attack; $\varepsilon = \sqrt{v^2 + w^2}/V$	–

TABLE 5. AERODYNAMIC COEFFICIENTS AND THEIR POLYNOMIAL EXPANSIONS

SYMBOL	DEFINITION AND EXPANSION*
$\bar{C}_X$	Axial force coefficient; $\bar{C}_X = C_X + C_{X2}\varepsilon^2 + C_{XV}\ (V_0-V)$
$\bar{C}_{N\alpha}$	Normal force coefficient slope; $\bar{C}_{N\alpha} = C_{N\alpha} + C_{N\alpha 3}\varepsilon^2$
$\bar{C}_{Yp\alpha}$	Magnus force coefficient slope; $\bar{C}_{Yp\alpha} = C_{Yp\alpha} + C_{Yp\alpha 3}\varepsilon^2$
$\bar{C}_{m\alpha}$	Pitching moment coefficient slope; $\bar{C}_{m\alpha} = C_{m\alpha} + C_{m\alpha 3}\varepsilon^2 + C_{m\alpha V}\ (V_0-V)$
$\bar{C}_{mq}$	Damping moment coefficient; $\bar{C}_{mq} = C_{mq} + C_{mq2}\varepsilon^2$
$\bar{C}_{np\alpha}$	Magnus moment coefficient slope; $\bar{C}_{np\alpha} = C_{np\alpha} + C_{np\alpha 3}\varepsilon^2$
C_{lp}	Spin deceleration coefficient
$C_{l\delta}$	Fin cant moment coefficient
C_I	Moment of inertia ratio coefficient; $C_I = 1$

*ε is the sine of the total angle-of-attack.

Given the variables and constants defined in Tables 2 through 5, the twelve state dynamic equations can be written as shown in Table 6. The moment of inertia ratio coefficient, C_I, used in Equation 11 in Table 6 is equal to one in any real system. However, the filter can estimate the ratio I_x/I_y more accurately than it can be measured. Since a measured value of I_x/I_y is used in the filter implementation, the estimate of C_I adjusts for the error in this measured quantity.

TABLE 6. EQUATIONS OF MOTION

NO.	EQUATION
1.	$\dot{x} = u\cos\theta\cos\psi - v\sin\psi + w\sin\theta\cos\psi$
2.	$\dot{y} = u\cos\theta\sin\psi + v\cos\psi + w\sin\theta\sin\psi$
3.	$\dot{z} = -u\sin\theta + w\cos\theta$
4.	$\dot{u} = -\left(\frac{\bar{q}A}{m}\right)\bar{C}_X + g\sin\theta - \dot{\theta}w + \dot{\psi}v\cos\theta$
5.	$\dot{v} = -\left(\frac{\bar{q}A}{m}\right)\bar{C}_{N\alpha}\frac{v}{V} + \left(\frac{\bar{q}A}{m}\right)\left(\frac{pd}{2V}\right)\bar{C}_{Yp\alpha}\frac{w}{V} - \dot{\psi}(u\cos\theta + w\sin\theta)$
6.	$\dot{w} = -\left(\frac{\bar{q}A}{m}\right)\bar{C}_{N\alpha}\frac{w}{V} - \left(\frac{\bar{q}A}{m}\right)\left(\frac{pd}{2V}\right)\bar{C}_{Yp\alpha}\frac{v}{V} - g\cos\theta + \dot{\psi}v\sin\theta + \dot{\theta}u$
7.	$\dot{\psi} = \dot{\psi}$
8.	$\dot{\theta} = \dot{\theta}$
9.	$\dot{\phi} = p + \dot{\psi}\sin\theta$
10.	$\ddot{\psi} = \left\{-\left(\frac{\bar{q}Ad}{I_y}\right)\bar{C}_{m\alpha}\frac{v}{V} + \left(\frac{\bar{q}Ad}{I_y}\right)\left(\frac{d}{2V}\right)\bar{C}_{mq}\dot{\psi}\cos\theta + \left(\frac{\bar{q}Ad}{I_y}\right)\left(\frac{pd}{2V}\right)\bar{C}_{np\alpha}\frac{w}{V} + 2\dot{\theta}\dot{\psi}\sin\theta + \dot{\theta}p\,C_I\left(\frac{I_x}{I_y}\right)\right\}\frac{1}{\cos\theta}$
11.	$\ddot{\theta} = \left(\frac{\bar{q}Ad}{I_y}\right)\bar{C}_{m\alpha}\frac{w}{V} + \left(\frac{\bar{q}Ad}{I_y}\right)\left(\frac{d}{2V}\right)\bar{C}_{mq}\dot{\theta} + \left(\frac{\bar{q}Ad}{I_y}\right)\left(\frac{pd}{2V}\right)\bar{C}_{np\alpha}\frac{v}{V} - \dot{\psi}p\cos\theta\,C_I\left(\frac{I_x}{I_y}\right) - \dot{\psi}^2\cos\theta\sin\theta$
12.	$\dot{p} = \left(\frac{\bar{q}Ad}{I_x}\right)\left(\frac{d}{2V}\right)C_{lp}p + \left(\frac{\bar{q}Ad}{I_x}\right)C_{l\delta}$

This completes the definition of the system dynamic model. The model is used to generate projectile trajectories from which measurements are derived to be applied to the filter; it is also used as the mathematical model upon which the filter design is based.

The measurement model takes noisy measurements of position and angular orientation (x,y,z,ψ,θ, and ϕ) and time as the projectile passes 50 downrange measurement stations during its flight. To each of these quantities, a random gaussian uncorrelated noise sequence is added with a given rms value.

3.2 EXTENDED KALMAN FILTER ALGORITHM DESIGN

In this section, the EKF algorithm summarized in subsection 2.2 is applied to estimate the 17 aerodynamic coefficients contained in the system model defined in subsection 3.1. To do this, the system model must be put into the form of Equations (12) and (13). Let the 12 dynamic state variables listed in Table 2 be brought together, in the order listed, into the vector $\underline{y}$, and let the 17 constant aerodynamic coefficients form the vector $\underline{a}$. Then the equations of motion listed in Table 6 can be expressed in state vector notation as

$$\dot{\underline{y}} = \underline{g}(\underline{y},\underline{a}) \tag{18}$$

where $\underline{g}$ is a nonlinear vector function of $\underline{y}$ and $\underline{a}$. Since the unknown coefficients contained in $\underline{a}$ are assumed to be constant, the dynamic model for $\underline{a}$ is given by

$$\dot{\underline{a}} = \underline{0} \tag{19}$$

where $\underline{0}$ is the zero vector.

To apply the EKF algorithm, all of the quantities to be estimated in Equation (18) must be expressed in state variable form. This is readily accomplished by augmenting Equation (18) with Equation (19) as follows:

$$\begin{bmatrix} \dot{\underline{y}} \\ \dot{\underline{a}} \end{bmatrix} = \begin{bmatrix} \underline{g}(\underline{y},\underline{a}) \\ \underline{0} \end{bmatrix} \tag{20}$$

Equation (20) is a special case of Equation (12) where

$$\underline{x} = \begin{bmatrix} \underline{y} \\ \underline{a} \end{bmatrix}; \quad \underline{f}(\underline{x},t) = \begin{bmatrix} \underline{g}(\underline{y},\underline{a}) \\ \underline{0} \end{bmatrix} \tag{21}$$

and

$$G(t)\underline{w}(t) = \underline{0} \tag{22}$$

The measured quantities in this application are system states except for the time measurement. Thus, the state measurements are linear, and Equation (13) can be expressed as

$$\underline{z}_k = H_k\underline{x}(t_k) + \underline{v}_k \qquad k=1,2,\ldots,50 \tag{23}$$

where t_k is the measured measurement time and $\underline{z}_k$ are the noisy measured values of x, y, z, ψ, θ, and ϕ. For this case, the H_k matrix is time-invariant and given by

$$H_k = \left[\begin{array}{ccccccccc:c} 1 & 0 & 0 & 0 & 0 & 0 & 0 & 0 & 0 & \\ 0 & 1 & 0 & 0 & 0 & 0 & 0 & 0 & 0 & \\ 0 & 0 & 1 & 0 & 0 & 0 & 0 & 0 & 0 & \\ 0 & 0 & 0 & 0 & 0 & 0 & 1 & 0 & 0 & [0]_{6\times 20} \\ 0 & 0 & 0 & 0 & 0 & 0 & 0 & 1 & 0 & \\ 0 & 0 & 0 & 0 & 0 & 0 & 0 & 0 & 1 & \end{array}\right] \tag{24}$$

The vector $\underline{v}_k$ in Equation (23) represents the measurement noise and consists of the combined effect of the position and time measurement errors. Since the random time measurement error, ε_t, is very small for this application (0.5 μsec rms), the projectile velocities can be assumed constant over the error interval and the total measurement error is approximated by

$$\underline{v}_k = \underline{v}'_k - H_k\dot{\underline{x}}(t_k)\varepsilon_t \tag{25}$$

The covariance of $\underline{v}_k$ is thus given by

$$R_k = R'_k + H_k\, E\left[\dot{\underline{x}}(t_k)\dot{\underline{x}}(t_k)^T\right]H_k^T\,\sigma_t^2 \tag{26}$$

where $\underline{v}'_k$ is the measurement error without time measurement error, R'_k its covariance matrix, and σ_t the rms value of the time measurement error. For the current application, the second term on the right-hand side of Equation (26) is significant only in the measurement of the projectile roll angle, which changes at a high angular rate. Consequently, R_k is assumed equal to R'_k except for the diagonal element associated

with the roll-angle measurement error, which is approximated by

$$R_k(6,6) \cong R'_k(6,6) + \hat{p}^2 \sigma_t^2 \qquad (27)$$

where $\hat{p}$ is the estimate of projectile spin rate. The validity of this approximation is demonstrated by the results presented in Section IV of this report.

Before presenting the performance and sensitivity results, a few specific implementation details should be discussed. First, the filter design is based upon the correct values of the projectile constants, d, I_x, I_y, m, and g. Normally each of these quantities will be measured off-line with some errors. Except for the ratio I_x/I_y, none of the projectile constants can be estimated by the filter independently from the aerodynamic coefficients. For example, in Equation 4 of Table 6, $\overline{C}_X$ is estimated by assuming that the value of A/m is known. In practice, the filter can estimate only the combination, A/m $\overline{C}_X$, *not* $\overline{C}_X$ and A/m individually. In this sense, the problem is over parameterized, and all measured or unknown quantities cannot be estimated independently. Therefore, for convenience any measurement errors in the projectile parameters are attributed to uncertainty in the aerodynamic coefficients, in order to maintain the explicit form of the equations of motion in Table 6.

Second, the assumption of a flat non-rotating earth is not valid for data generated in a ballistic range and must be accounted for in an operational program. Third, the computation of the $F(\hat{\underline{x}}(t),t)$ matrix in Table 1 requires the computation of

$$F(\underline{x},t) = \frac{\partial \underline{f}(\underline{x},t)}{\partial \underline{x}(t)} \qquad (28)$$

This matrix of partial derivatives is explicitly derived for the filter's implementation. The only assumption made in this derivation is that the air density, ρ, is independent of altitude, z. While not strictly correct, the error induced by this approximation is trivial. Appendix A gives the detailed equations used to compute this matrix.

Finally, the initialization procedure is very important to the proper operation of the filter. Before the first measurement, only very rough a priori estimates of the

projectile's position and downrange velocity at the first measurement station are available. Thus, the angular and translational position and velocity initial estimates are set to zero or nominal values for this station, and their error covariances are initialized at correspondingly high values. The coefficient estimates and their error covariances are initialized based upon the a priori knowledge of the projectile's aerodynamic properties. Based on these initial conditions, the first measurement set is processed, and the filter estimate and its covariance are updated. This single measurement of six positions brings the error covariance of the position estimate down to the measurement noise level but provides no information on the six velocities at the first station. Thus, the velocity estimates remain extremely poor.

The filter estimates and covariance are propagated to the next measurement time, and the second filter update is performed using the second measurement set. This greatly improves the estimates of the six projectile velocities because two sets of accurate position measurements at different times have been processed. However, the error covariance at this point has not been computed correctly. Recall that the EKF design requires a linearization about the state estimate to propagate the error covariance between two measurements. Between the first and second measurements the velocity estimates are very inaccurate, resulting in a poor linearization. Consequently, the covariance after the second measurement is not a good reflection of the true error covariance. This problem must be corrected at the second measurement if future measurements are to be processed correctly.

The following filter resetting procedure was found to be a satisfactory method of correcting the problem described above. Immediately after the second measurement update, the filtering problem is essentially restarted by resetting the error covariance matrix as follows: the error covariance matrix off diagonal elements are all set to zero; the diagonal elements corresponding to positions are reset to the measurement noise levels for those positions; the diagonal elements corresponding to coefficient estimates are set to their original values assumed before the first measurement; the diagonal element corresponding to the velocity along the projectile axis of symmetry is unchanged; and the diagonal elements corresponding to the other two translational velocities and the three angular velocities are increased by a factor of ten over their current values. This covariance matrix is then propagated together with the estimate to the third measurement, the third update occurs, and normal processing continues thereafter. Since the estimates of position and velocity are fairly accurate after the reset, the linearization is good over the propagation between the reset and the

third measurement and the filter operates properly, correctly computing the estimates and their corresponding error covariance matrix. Essentially, the reset starts the filter over after the second measurement update with a new initial covariance matrix that is a much more accurate representation of true velocity estimation errors. The effectiveness of this initialization procedure is demonstrated by the experimental results presented in Section IV.

SECTION IV

PERFORMANCE AND SENSITIVITY RESULTS

This section presents performance and sensitivity results obtained using the EKF algorithm described in subsection 3.2. Test procedures and performance measures are discussed, a nominal test case is defined, and the filter performance for this case is demonstrated. Finally, sensitivities to variations in the nominal test conditions are investigated.

4.1 TEST PROCEDURES AND PERFORMANCE MEASURES

Experimental data is generated by a trajectory simulation program which integrates the equations of motion given in Table 6, based on given true values for all the components of the model. As the downrange position of the projectile reaches each measurement station, the time, position, and angular orientation of the projectile are computed and corrupted by independent zero-mean gaussian noise sequences. Thus, the input data to the filter consists of 50 sets of seven measurements (three angular positions, three translational positions, and time). The filter design is specified by the system model and its constants. It begins with a given initial state estimate $\underline{x}_0$ and an assumed covariance matrix, P_0.

The performance of the filter is evaluated by observing its estimation error in relation to the error standard deviations obtained from the covariance matrix computation. If the errors are consistent with the computed standard deviation, then the filter is considered to be operating properly and its absolute performance can be judged by the estimation errors achieved. Thus, there are two basic measures of performance, estimation error and consistency between this error and its computed standard deviation.

4.2 THE NOMINAL CASE

The nominal trajectory is obtained by integration of the equations of motion in Table 6, using the projectile constants listed in Table 7, the trajectory dynamic initial conditions (at t=0) listed in Table 8, and the true aerodynamic coefficient values listed in Table 9. As the downrange position (x) of the projectile passes the 50 measurement station locations listed in Table 10, measurements of time, angular position, and translational position are made. These

TABLE 7. NOMINAL PROJECTILE CONSTANTS

SYMBOL	DESCRIPTION	NOMINAL VALUE
d	Diameter	9.8333×10^{-2} ft (33 mm)
m	Mass	2.4865×10^{-2} slug (0.80 #)*
I_x	Axial moment of inertia	3.2376×10^{-5} slug-ft^2 (0.15 # in.^{2})
I_y	Transverse moment of inertia	2.6764×10^{-4} slug-ft^2 (1.24 # in.^{2})
V_0	Reference velocity	3.3457×10^{3} ft/sec (Mach 3.00)

*32.174 # = 1 slug

TABLE 8. TRAJECTORY GENERATOR AND FILTER DYNAMIC STATE INITIAL CONDITIONS

DYNAMIC STATE	UNITS	TRAJECTORY MODEL INITIAL CONDITION; $t=0$	TRUE VALUE AT FIRST MEASUREMENT STATION; $t=t_1$	INITIAL VALUE ASSUMED BY FILTER AT $t=t_1$	RMS ERROR ASSUMED BY FILTER AT $t=t_1$
x	ft	0.0	5.03	5.0	1.0
y	ft	0.0	1.31×10^{-4}	0.0	1.0
z	ft	20.0	20.008	20.0	1.0
u	ft/sec	3,351.0	3,340.7	3,000.0	600.0
v	ft/sec	0.0	-201.0	0.0	300.0
w	ft/sec	0.0	137.2	0.0	300.0
ψ	rad	0.0	0.060	0.0	1.0
θ	rad	-1.745×10^{-3}	0.040	0.0	1.0
ϕ	rad	0.0	16.05	0.0	200.0
$\dot{\psi}$	rad/sec	0.0	56.85	0.0	100.0
$\dot{\theta}$	rad/sec	55.0	-18.11	0.0	100.0
p	rad/sec	10,703.0	10,700.8	10,000.0	1,000.0

TABLE 9. TRUE COEFFICIENT VALUES, INITIAL FILTER ESTIMATES, AND INITIAL ASSUMED STANDARD DEVIATIONS OF ERRORS

AERODYNAMIC COEFFICIENT	TRUE VALUE	INITIAL FILTER ESTIMATE	RMS ERROR IN INITIAL ESTIMATE ASSUMED BY FILTER	INITIAL PERCENT ERROR
C_X	0.225	0.300	0.2	33
C_{X2}	1.5	0.0	1.0	-100
C_{XV}	-0.54×10^{-4}	0.0	1.0×10^{-4}	-100
$C_{N\alpha}$	2.87	2.75	0.32	-4
$C_{N\alpha3}$	10.0	0.0	5.0	-100
$C_{Yp\alpha}$	-0.9	-1.0	0.1	11
$C_{Yp\alpha3}$	5.0	0.0	3.0	-100
$C_{m\alpha}$	3.15	2.50	0.75	-21
$C_{m\alpha3}$	-6.0	0.0	6.0	-100
$C_{m\alpha V}$	2.58×10^{-4}	0.0	3.0×10^{-4}	-100
C_{mq}	-18.0	-15.0	5.0	-17
C_{mq2}	10.0	0.0	5.0	-100
$C_{np\alpha}$	0.3	0.0	1.0	-100
$C_{np\alpha3}$	2.0	0.0	2.0	-100
C_{lp}	-0.024	-0.015	0.015	-38
$C_{l\delta}$	-1.0×10^{-3}	0.0	1.0×10^{-3}	-100
C_I	1.00	1.01	0.01	1

TABLE 10. MEASUREMENT STATION LOCATIONS

STATION NUMBER	DOWNRANGE POSITION (FT)	STATION NUMBER	DOWNRANGE POSITION (FT)
1	5	26	275
2	15	27	290
3	25	28	305
4	35	29	320
5	45	30	335
6	55	31	350
7	65	32	380
8	75	33	395
9	85	34	410
10	95	35	425
11	115	36	440
12	125	37	445
13	135	38	470
14	145	39	485
15	155	40	500
16	170	41	515
17	180	42	530
18	190	43	545
19	210	44	560
20	220	45	585
21	230	46	600
22	240	47	615
23	250	48	630
24	260	49	645
25	270	50	660

measurements consist of the true values of these quantities corrupted by independent sequences of uncorrelated zero-mean gaussian noise samples. The standard deviations of the noise sequences for the measurement of position (translational and angular) and time are given in Table 11. Figures 5 and 6 are plots of some of the states of the nominal trajectory to illustrate its general form and frequency content. Figure 6 also includes a plot of the total angle-of-attack, $\bar{\alpha}$, defined by

$$\bar{\alpha} = \sin^{-1}(\varepsilon) = \sin^{-1}\left[\frac{\sqrt{v^2 + w^2}}{V}\right] \qquad (29)$$

This trajectory represents a model of a 30mm projectile traveling at approximately Mach 3 with initial Euler angle rates of $\dot{\theta}(0) = 55$ radians per second and $\dot{\psi}(0) = 0$ radians per second.

The filter design is based upon the same equations of motion and projectile constants as the nominal trajectory. The filter is initialized at time t_1 when the projectile activates the first measurement station. Table 8 gives the true values of the projectile dynamic states at t_1, the initial filter estimates, and the initial rms errors in the estimates assumed by the filter at time t_1. Note that only rough knowledge of the initial positions and velocities is assumed by the filter.

TABLE 11. NOMINAL MEASUREMENT ERROR STANDARD DEVIATIONS

SYMBOL	DESCRIPTION	NOMINAL VALUE
σ_p	Translational Position (x,y,z) Measurement Error Standard Deviation	0.01 ft (~0.1 in.)
σ_a	Angular Orientation (ψ,θ,ϕ) Measurement Error Standard Deviation	1.73×10^{-3} rad (0.1 deg)
σ_t	Time of Measurement Error Standard Deviation	0.5 μsec

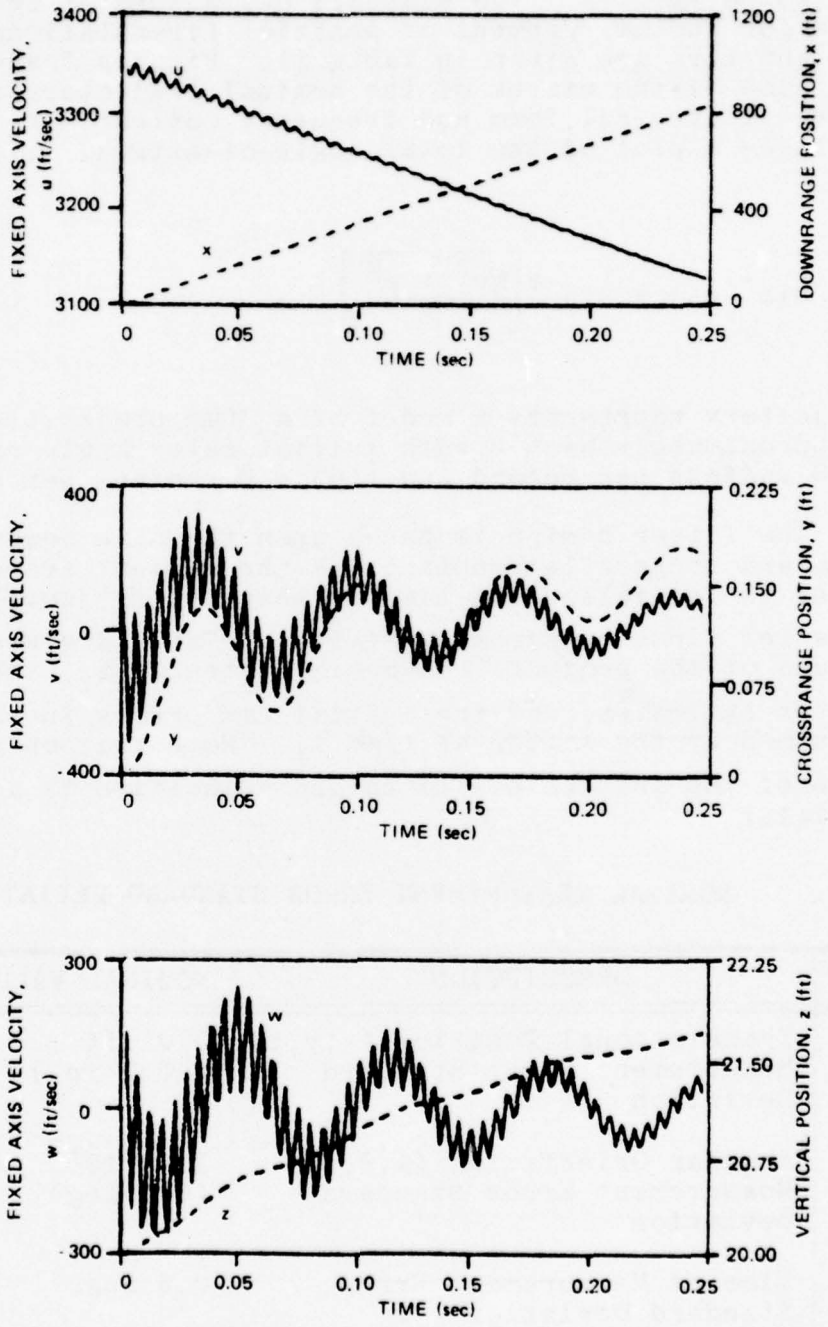

Figure 5. Nominal Trajectory States x, y, z, u, v, and w

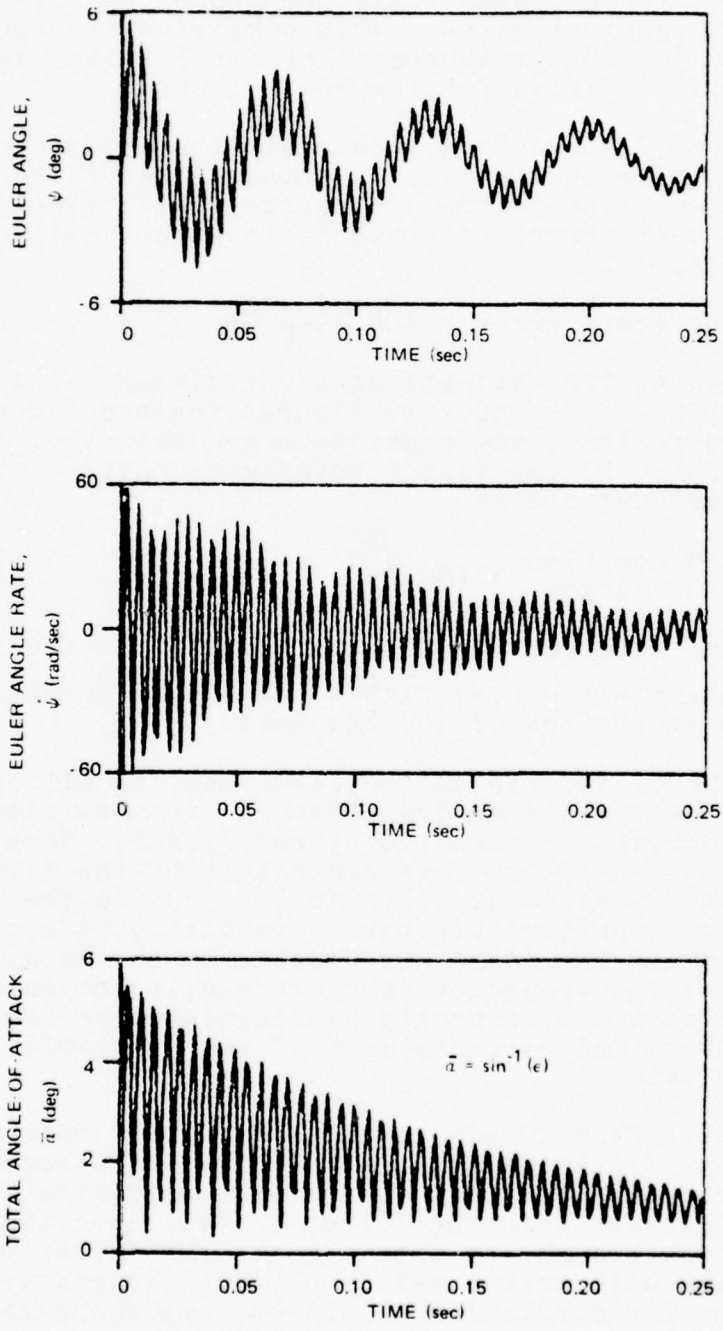

Figure 6. Nominal Trajectory States ψ, $\dot{\psi}$, and Total Angle-of-Attack $\bar{\alpha}$

In a similar manner, Table 9 gives the true values of the 17 aerodynamic coefficients, the initial values of the coefficient estimates, and the rms estimation errors assumed by the filter. Table 9 also lists the percent errors in the initial coefficient estimates. This completes the specification of the trajectory, measurement process, filter design, and filter initialization for the nominal case.

Figures 7 through 13 illustrate the coefficient estimation error performance of the extended Kalman filter for the nominal case. The estimation errors (solid lines) are plotted as percent errors relative to the true coefficient values, that is,

$$\text{Percent estimate error} = 100\,\frac{(\hat{C} - C)}{C} \tag{30}$$

where $\hat{C}$ represents the estimate of a coefficient, C its true value. Also plotted on the same figures (dashed lines) are the normalized positive and negative one-σ values of these errors as computed by the filter covariance matrix. These one-σ values are defined as

$$\text{Normalized computed standard deviation} = 100\,\frac{\sqrt{P_C}}{C} \tag{31}$$

where P_C is the value of the diagonal element in the filter covariance matrix associated with C. Table 12 summarizes the filter errors at the end of the trajectory.

Figures 7 through 13 indicate that, in all cases, the parameter estimation errors achieved are consistent with the standard deviations computed by the filter. Some of the coefficients are estimated very accurately by the filter while others are not estimated at all. This is due to the fact that some of the coefficients have very little effect on the trajectory and are therefore not visible in the data. Others strongly affect the trajectory and are easily estimated. The covariance calculation correctly distinguishes between these coefficient types and extracts most of the available information from the data.

An attempt was made to improve the estimates for the nominal case by filtering the nominal data set a second time. This was done using the final coefficient estimates and their respective covariances as the filter initial condition for the second pass through the data. Since the filter begins the second pass with better estimates, the linearization assumed in the EKF derivation should be more accurate, and the filter should be closer to an optimum design. Table 12 lists the results of this experiment, designated Test No. 1,

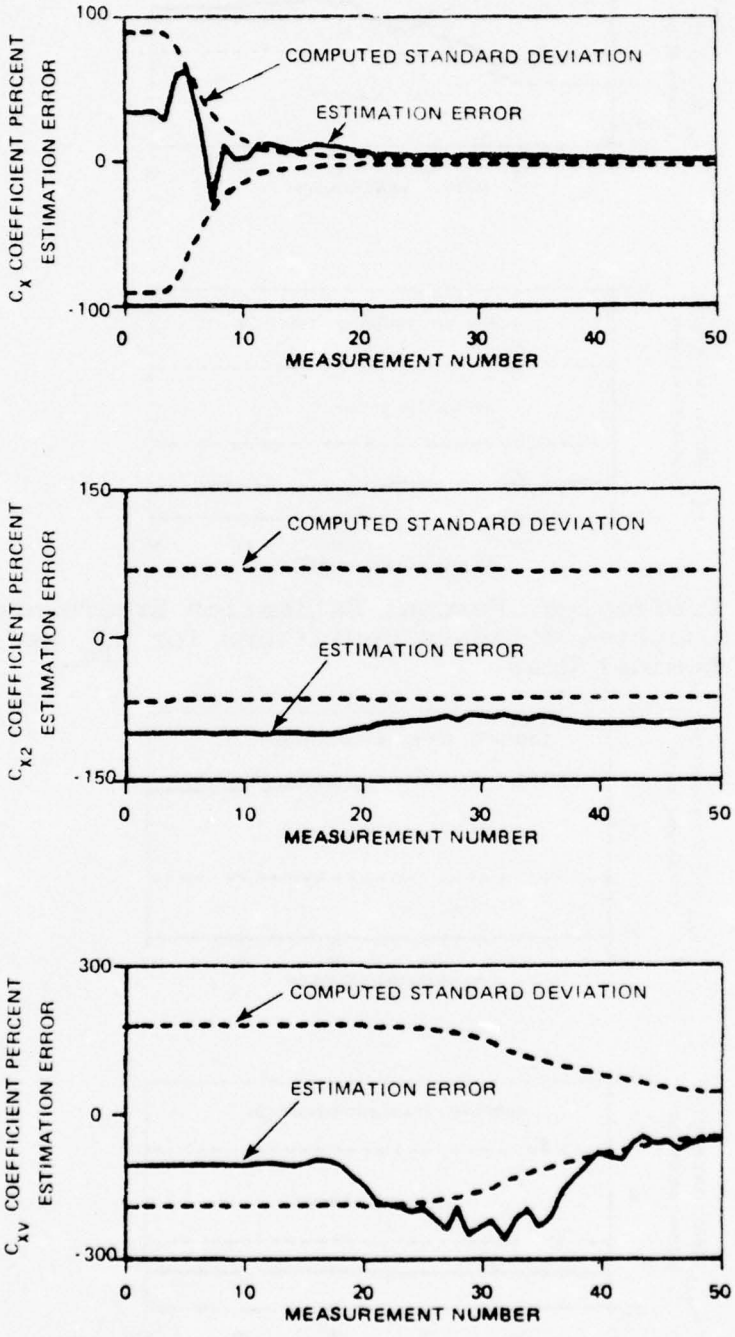

Figure 7. Coefficient Percent Estimation Errors and Their Computed Standard Deviations for C_X, C_{X2}, and C_{XV}; Nominal Case

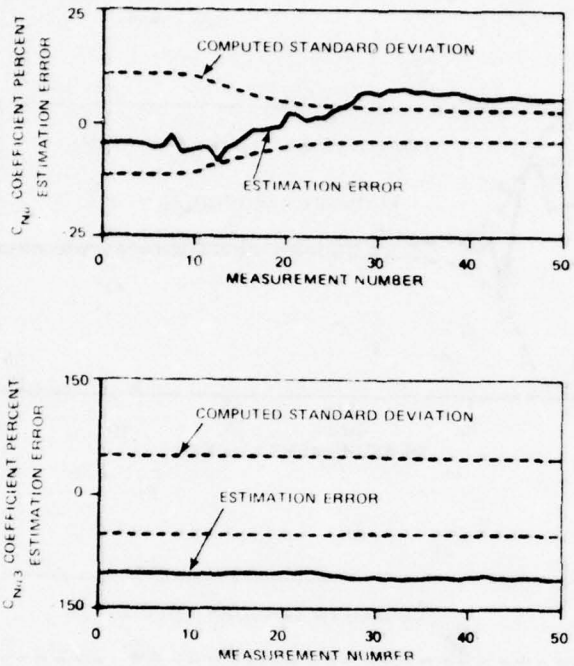

Figure 8. Coefficient Percent Estimation Errors and Their Computed Standard Deviations for $C_{N\alpha}$ and $C_{N\alpha 3}$; Nominal Case

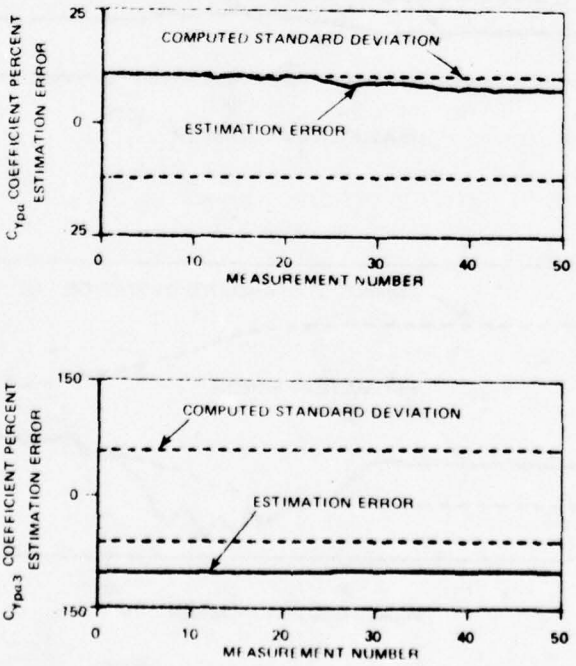

Figure 9. Coefficient Percent Estimation Errors and Their Computed Standard Deviations for $C_{Yp\alpha}$ and $C_{Yp\alpha 3}$; Nominal Case

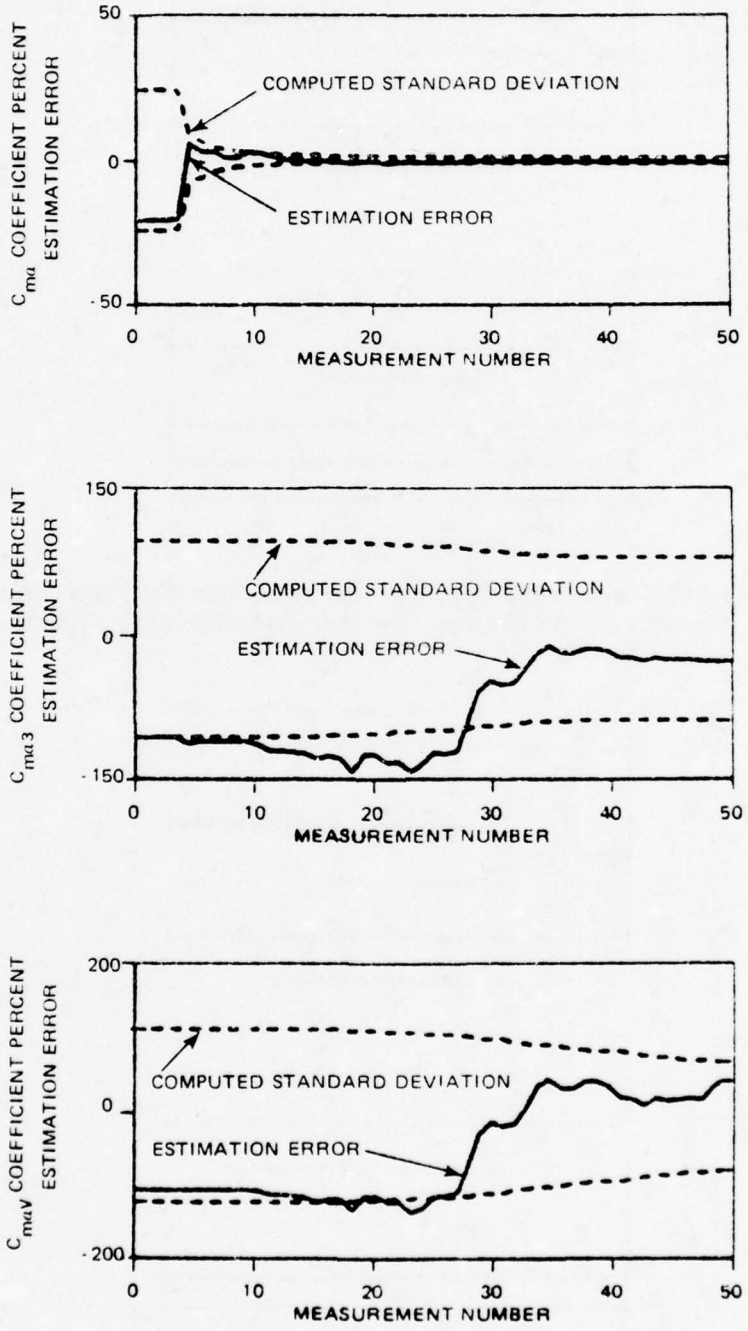

Figure 10. Coefficient Percent Estimation Errors and Their Computed Standard Deviations for $C_{m\alpha}$, $C_{m\alpha 3}$, and $C_{m\alpha V}$; Nominal Case

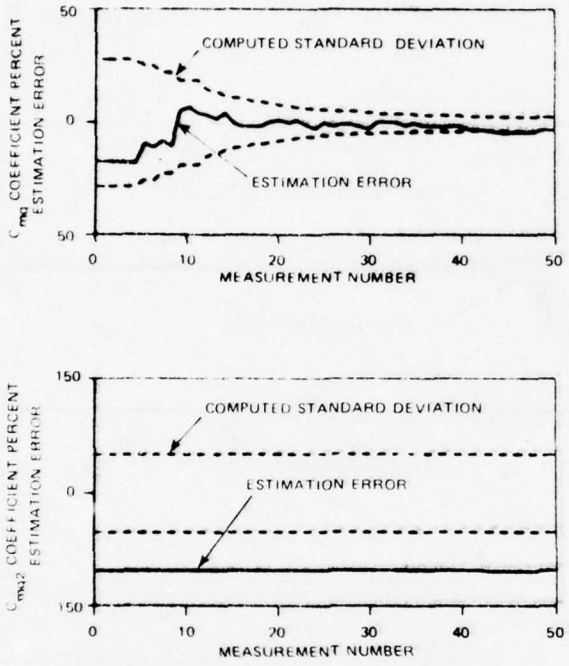

Figure 11. Coefficient Percent Estimation Frrors and Their Computed Standard Deviations for C_{mq} and C_{mq2}: Nominal Case

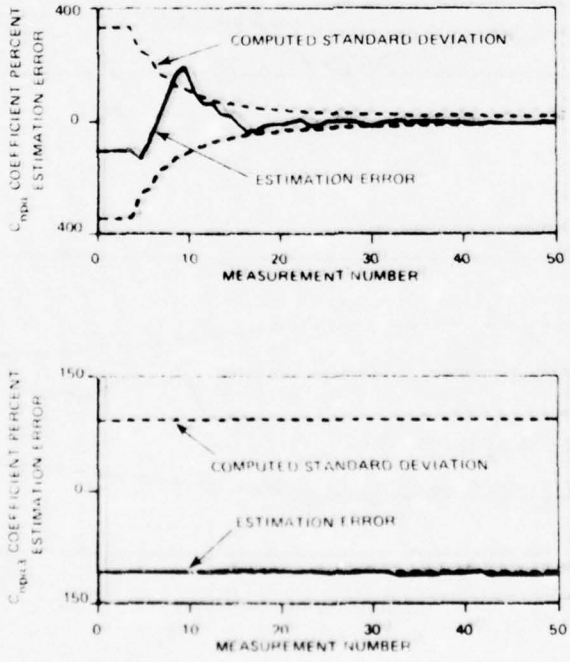

Figure 12. Coefficient Percent Estimation Errors and Their Computed Standard Deviations for $C_{np\alpha}$ and $C_{np\alpha3}$: Nominal Case

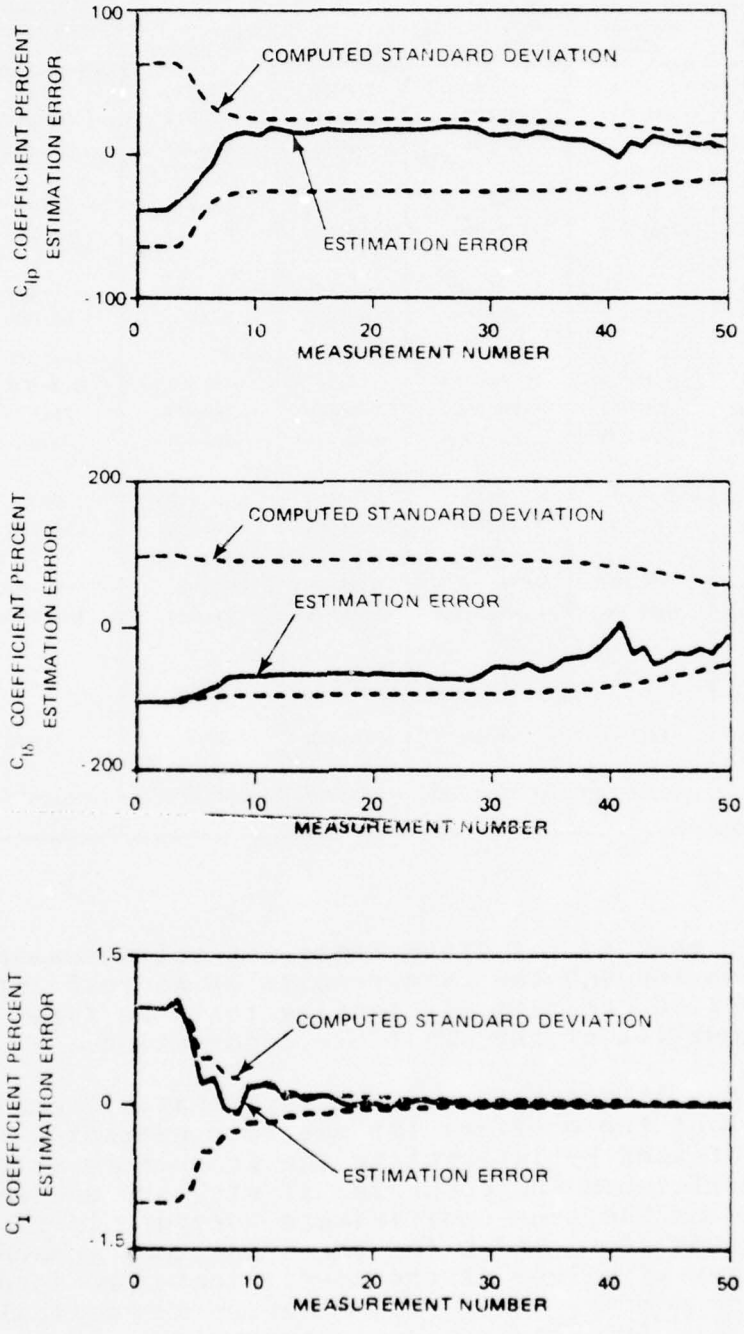

Figure 13. Coefficient Percent Estimation Errors and Their Computed Standard Deviations for C_{lp}, $C_{l\delta}$, and C_I; Nominal Case

TABLE 12. FILTER PERFORMANCE TEST RESULTS

AERODYNAMIC COEFFICIENT	PERCENT ERROR AND (NORMALIZED STANDARD DEVIATION)						
	INITIAL CONDITIONS	NOMINAL CASE	TEST NO. 1 DOUBLE PASS	TEST NO. 2 $\hat{A}(0)=0$	TEST NO. 3 $\hat{A}(0)=100$	TEST NO. 4 $\sigma_I=0$	TEST NO. 5 HIGH NOISE
C_X	23(89)	2(2)	2(1.5)	0.2(0.6)	4(4)	2(2)	4(3)
C_{X2}	-100(67)	-91(61)	-81(63)	-100(67)	-52(51)	-91(64)	-99(65)
C_{XV}	-100(185)	-61(45)	-53(40)	-11(29)	-102(90)	61(45)	101(89)
C_{N_α}	-4(11)	6(3)	6(2)	-5(11)	6(2)	6(3)	12(7)
$C_{N\alpha 3}$	-106(50)	-103(50)	-112(49)	100(50)	-105(41)	-105(50)	-99(50)
$C_{Yp\alpha}$	11(31)	8(11)	6(11)	11(-1)	6(11)	8(11)	10(11)
$C_{Yp\alpha 3}$	100(60)	-97(60)	-95(60)	100(60)	86(60)	98(60)	-99(60)
C_{m_α}	-21(24)	-0.4(0.8)	-0.6(0.8)	11(9)	0.6(1.1)	-0.4(0.8)	-0.3(1)
$C_{m\alpha 3}$	-100(100)	-21(82)	-26(79)	-100(100)	16(37)	-25(82)	-38(92)
C_{mV}	-100(117)	18(73)	66(67)	102(116)	-19(89)	46(73)	8(99)
C_{mq}	-17(28)	-2(3)	-3(2)	-18(28)	-0.8(1.5)	-2(3)	-1(8)
C_{mq2}	-100(50)	-100(50)	-101(50)	-100(50)	-96(19)	100(50)	-100(50)
$C_{np\alpha}$	-100(333)	10(12)	-11(9)	260(295)	-0.2(9)	-9(12)	-18(31)
$C_{np\alpha 3}$	-100(100)	-102(100)	-106(99)	-100(100)	-67(91)	-103(100)	-101(100)
C_{lp}	-38(63)	1(11)	1(11)	-2(6)	2(5)	-2(6)	1(16)
$C_{l\delta}$	-100(100)	-11(56)	-3(13)	6(23)	6(50)	7(23)	-3(59)
C_l	1(1)	-0.01(0.02)	-0.01(0.015)	1(0.9)	-0.01(0.011)	0.01(0.02)	-0.03(0.06)

as well as the results for other tests not yet discussed. The second pass through the data results in no real improvement in estimation accuracy, indicating that the first pass extracted almost all of the available information.

Another illustration of the fact that all pertinent information about the coefficients has been extracted from the data is obtained by integrating the trajectory using the estimated coefficients and comparing it with the nominal trajectory based on the true coefficients. Figure 14 shows the trajectory states y, v, and ψ for the trajectory generated using the estimated values of the coefficients provided by the EKF for the nominal case. These curves are virtually indistinguishable from their true counterparts in Figures 5 and 6.

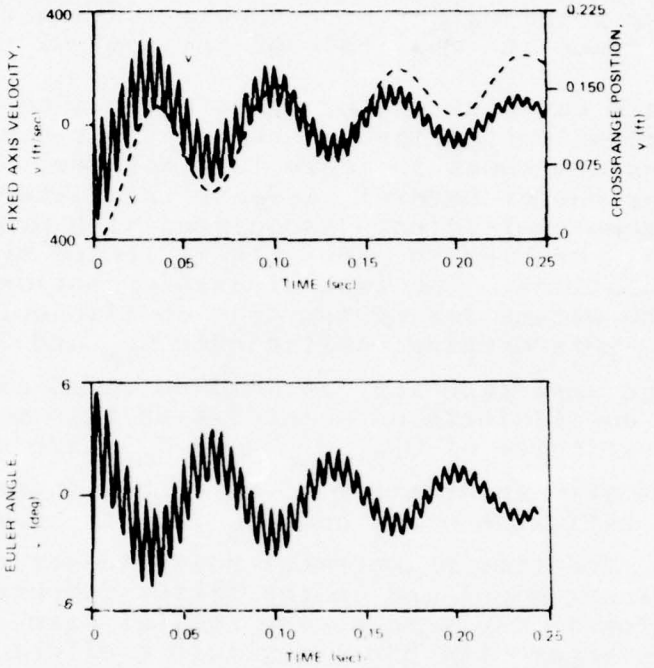

Figure 14. States y, v, and ψ for the Trajectory Based on the Estimated Aerodynamic Coefficients for the Nominal Case

4.3 PERFORMANCE SENSITIVITY TO TRAJECTORY AND MEASUREMENT ERROR LEVEL

Table 12 summarizes the performance of the EKF for the nominal case and several additional simulations. Tests No. 2 and No. 3 are designed to show the sensitivity of EKF performance to the amount of angular motion in the trajectory. The conditions for these two tests differ from the nominal case only in the initial conditions on the trajectory generator. Recall that for the nominal trajectory the initial Euler angle rates are

$\dot{\theta}(0)$ = 55 radians per second

$\dot{\psi}(0)$ = 0 radians per second

In Test No. 2, $\dot{\theta}(0)$ is set to zero resulting in a trajectory without the high frequency nutational motion seen in Figures 5 and 6. In Test No. 3, $\dot{\theta}(0)$ is set equal to 100 radians per second yielding a trajectory with a nutational motion of approximately twice the amplitude of the nominal trajectory.

In each case the filter operated in a consistent manner. The final estimation errors and their computed standard deviations are shown in Table 12. For Test No. 2, the lack of angular motion severely affects the filter's ability to estimate those coefficients associated with projectile nutations. This problem is correctly reflected by the covariance calculations. The lack of angular motion helps, however, in the estimation of the drag coefficients C_X and C_{XV} and in the spin damping coefficients C_{lp} and $C_{l\delta}$. Test No. 3 has large amplitude angular motions which aid in the estimation of coefficients associated with this motion. For example, the estimates of C_{X2}, C_{mq}, and $C_{m\alpha 3}$ are greatly improved. It is also interesting to note that there is a degradation in the estimates of C_X and C_{XV} from the nominal case. In Test No. 4, the time measurement noise is set to zero both in the measurement model and in the filter computations; otherwise, everything is the same as the nominal case. Time measurement noise apparently has a negligible effect on the estimation of all coefficients except those associated with the spin rate, C_{lp} and $C_{l\delta}$. Due to the high spin rate of about 10,000 radians per second, time errors look like increased roll position measurement errors as described in subsection 3.2. With no time measurement noise, the effective errors in roll angle measurement are smaller, thereby reducing the coefficient estimation errors.

In Test No. 5, the translational and angular position measurement noise variances are raised by a factor of ten. This change is made in both the measurement error model and in the filter design. As might be expected, the higher noise environment degrades the parameter estimates. In particular, the ability to estimate C_{XV} is almost lost, and those coefficients which were accurately estimated in the nominal case are generally degraded by factors of two or more in the higher noise environment. This effect is to be expected and it is accurately accounted for by the EKF's covariance calculation.

In summary, the study demonstrates that aerodynamic coefficient estimation accuracy is strongly influenced by the test scenario in which the filter operates. However, the EKF algorithm generally extracts most of the information about each coefficient available from the data and correctly assigns uncertainties to the estimates.

4.4 PERFORMANCE SENSITIVITY TO MODELING ERROR

In subsection 4.3, all of the experiments involve a filter design where the filter assumes the trajectory model actually used to generate the data. In many practical applications, the filter design model may only be an approximation to the system which generates the data. Such modeling error can severely affect the performance of the filtering algorithm. Table 13 summarizes the results of the nominal case and three experiments designed to test the effect of modeling error on filter performance.

TABLE 13. FILTER SENSITIVITY TEST RESULTS

	FINAL PERCENT ERROR AND (NORMALIZED STANDARD DEVIATION)				
AERODYNAMIC COEFFICIENT	INITIAL CONDITIONS	NOMINAL CASE	TEST NO. 6 σ_t UNMODELED	TEST NO. 7 C_{XV} AND $C_{m\alpha V}$ UNMODELED	TEST NO. 8 HIGH NOISE MODELING ERROR
C_X	33 (89)	2 (2)	2 (2)	-0.6 (0.5)	3 (2)
C_{X2}	-100 (67)	-91 (64)	-91 (64)	-138 (41)	-102 (65)
C_{XV}	-100 (185)	-61 (45)	-61 (45)	---	-73 (88)
$C_{N\alpha}$	-4 (11)	6 (3)	6 (3)	6 (3)	2 (7)
$C_{N\alpha 3}$	-100 (50)	-105 (50)	-105 (50)	-105 (50)	-99 (50)
$C_{Yp\alpha}$	11 (11)	8 (11)	8 (11)	8 (11)	11 (11)
$C_{Yp\alpha 3}$	-100 (60)	-97 (60)	-98 (60)	-97 (60)	-99 (60)
$C_{m\alpha}$	-21 (24)	-0.4 (0.8)	-0.4 (0.8)	-0.3 (0.3)	-0.1 (1)
$C_{m\alpha 3}$	-100 (100)	-24 (82)	-23 (82)	107 (55)	-62 (93)
$C_{m\alpha V}$	-100 (117)	48 (73)	51 (73)	---	-30 (99)
C_{mq}	-17 (28)	-2 (3)	-2 (3)	-2 (3)	-0.8 (8)
C_{mq2}	-100 (50)	-100 (50)	-100 (50)	-100 (50)	-100 (50)
$C_{np\alpha}$	-100 (333)	-10 (12)	-9 (12)	-10 (12)	-0.8 (34)
$C_{np\alpha 3}$	-100 (100)	-102 (100)	-102 (100)	-102 (100)	-100 (100)
C_{lp}	-38 (63)	4 (14)	-2 (6)	4 (14)	4 (15)
$C_{l\delta}$	-100 (100)	-14 (55)	9 (23)	-14 (55)	-17 (58)
C_l	1 (1)	-0.01 (0.02)	-0.01 (0.02)	-0.01 (0.02)	0.003 (0.06)

Test No. 6 investigates the influence of unmodeled time measurement noise. Here the filter assumes that the rms time measurement errors are zero when they are actually the same as for the nominal case. The effect of this modeling error is significant only in the estimates of those coefficients associated with the spin rate dynamics, C_{l_p} and C_{l_δ}. While the table seems to indicate performance improvement, this is not necessarily the case since the errors involved are random. Figure 15 shows the estimation error and standard deviation of C_{l_p} for the nominal case. Figure 16 shows them for Test No. 6; evidently the standard deviation is lower but the actual estimation error is larger. Thus, the average error performance is poorer than nominal, and the standard deviation gives a less conservative indication of the rms error. The same effect is shown in Figures 17 and 18 for C_{l_δ}. Figures 19 and 20 show the effect of this modeling error on the filter roll angle residual process. This process is defined to be the difference between each roll angle measurement and the value of that measurement predicted by the filter based upon past data. In these figures, the residuals are normalized by their computed standard deviations which are calculated from the filter covariance matrix. The residual process for Test No. 6 in Figure 20 has a much larger rms value than that for the nominal case shown in Figure 19. The fact that the rms normalized residuals in Figure 20 are so large is a good indication that modeling error exists in the roll dynamics or measurement model.

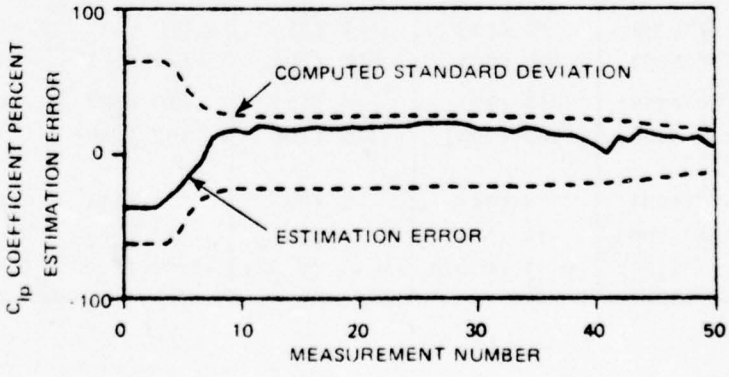

Figure 15. C_{l_p} Percent Estimation Error and Its Computed Standard Deviation; Nominal Case

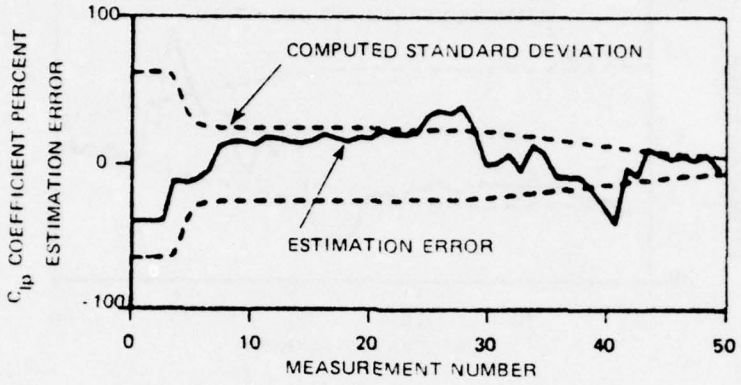

Figure 16. C_{lp} Percent Estimation Error and Its Computed Standard Deviation; Test No. 6 - Time Measurement Errors Unmodeled

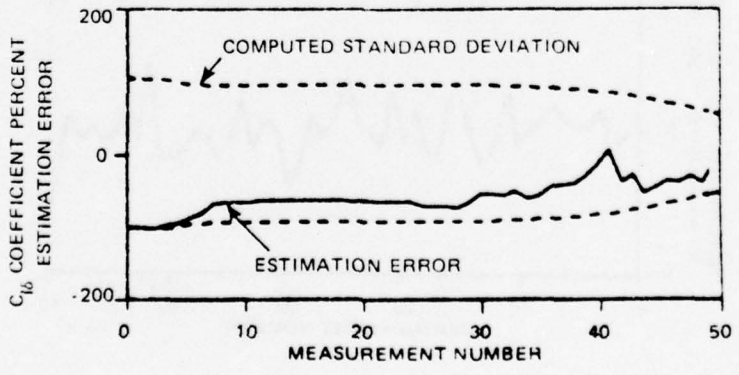

Figure 17. $C_{l\delta}$ Percent Estimation Error and Its Standard Deviation; Nominal Case

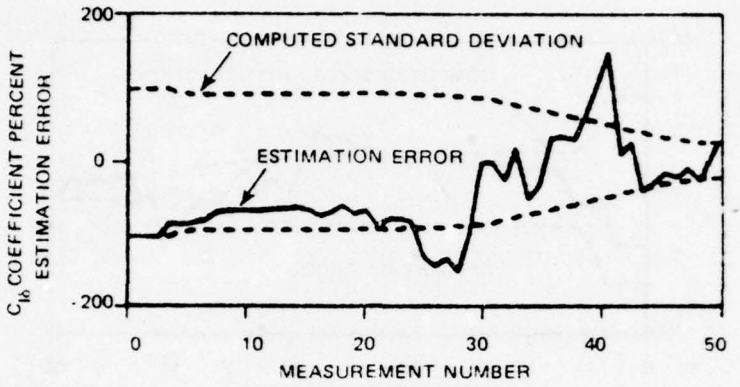

Figure 18. C_{l_δ} Percent Estimation Error and Its Standard Deviation; Test No. 6 - Time Measurement Errors Unmodeled

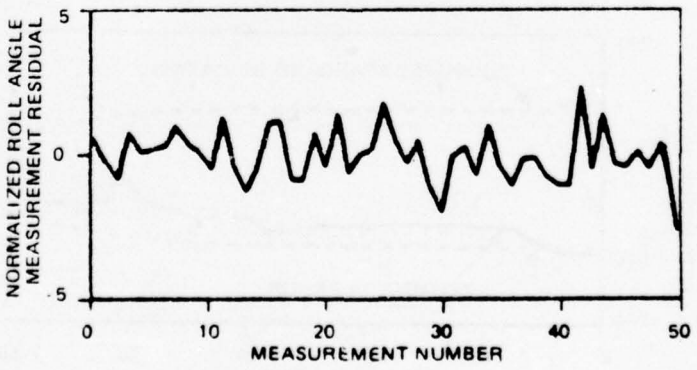

Figure 19. Normalized Roll Angle Measurement Residuals; Nominal Case

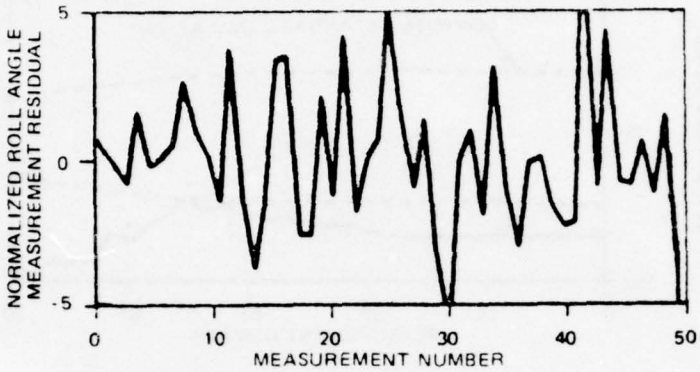

Figure 20. Normalized Roll Angle Measurement Residuals; Test No. 6 - Time Measurement Errors Unmodeled

Test No. 7 investigates the effect of not modeling the aerodynamic coefficients C_{XV} and $C_{m\alpha V}$, which account for changes in $\bar{C}_X$ and $\bar{C}_{m\alpha}$ as velocity changes. Figure 21 illustrates the effect of this modeling error on the estimates of C_{X2} and $C_{m\alpha 3}$; note the poor performance and apparent divergence as compared to the nominal case in Figures 7 and 10 where these estimates are much better behaved. Clearly, these velocity terms must be modeled by the filter if the aerodynamic coefficients change with velocity. Table 13 summarizes the results of this experiment.

Test No. 8 investigates the effect of the filter assuming rms position and angle measurement errors three times larger than actually exist. Table 13 shows that there is some degradation in performance, but it is not as large as might be expected. The computed standard deviations are overly conservative in this case, which might be desirable in a practical operational program.

4.5 DISCUSSION OF RESULTS

In the absence of significant modeling error, the EKF algorithm demonstrates excellent performance. While the design is known to be suboptimal because of the nonlinearities in the projectile dynamics, it appears that most of the significant information in the data is extracted by the algorithm; both the estimation errors and the measurement residuals are completely consistent with the rms values predicted by the

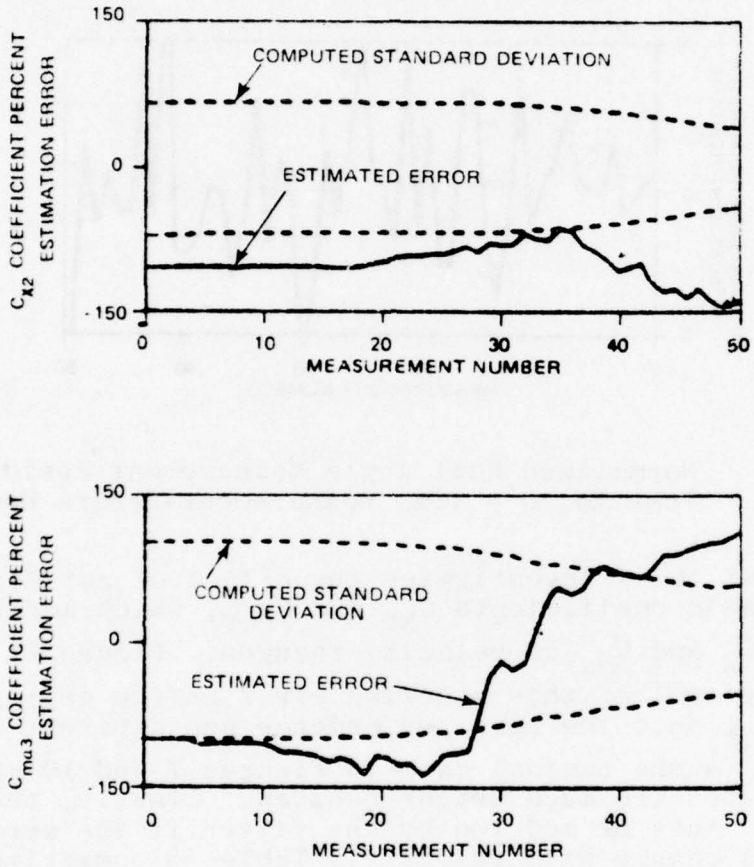

Figure 21. C_{X2} and $C_{m\alpha 3}$ Percent Estimation Errors and Their Computed Standard Deviations; Test No. 7 - C_{XV} and $C_{m\alpha V}$ Unmodeled

EKF covariance equations. For the nominal case, the linear drag coefficient C_X is estimated to within 2 percent and the drag variation with velocity C_{XV} to within 45 percent. The other force coefficients have only a minor influence on the trajectory and are not accurately estimated. The moment coefficient $C_{m\alpha}$ is estimated to within 1 percent; C_{mq} is estimated to within 3 percent, and $C_{np\alpha}$ to within 12 percent. The spin coefficient C_{lp} is obtained to within 14 percent and $C_{l\delta}$ to within 55 percent. Finally, the moment of inertia coefficient C_I is obtained to within 0.02 percent.

The algorithm is sensitive to modeling errors. This is reflected in the measurement residual processes. In processing test data, the residuals can indicate that the correct projectile model is not being used, thus helping in the development of a correct model for a given projectile. The EKF is also sensitive to the initial coefficient errors and the initial covariance matrix assumed for them. If these errors and/or their covariance are too large, the linearization assumed by the filter may be inadequate and the filter may operate poorly or diverge. Fortunately, engineering judgment in the initialization of the filter has been sufficient to insure good filter performance in this example.

The EKF algorithm requires the integration of the system states and the upper triangle of a 29 × 29 covariance matrix. This is done by trapezoidal integration at a step size of 0.05 millisecond. Larger step sizes lead to numerical instabilities and incorrect covariance propagation. The algorithm operates in approximately 300 thousand bytes of memory on an IBM-360-145, requiring 50 minutes of CPU time to process the 50 sets of measurement data. An operational algorithm could be developed which would improve these time and memory requirements considerably by elimination of unnecessary computations and storage and by improvements in the integration technique and program organization.

SECTION V

CONCLUSIONS

The principal conclusions of this report are:

1. The feasibility and accuracy of the extended Kalman filter for ballistic range aerodynamic coefficient extraction has been demonstrated for a 30mm projectile.

2. For the example used in this work, the EKF estimates 8 of the projectile's 17 aerodynamic coefficients to within 10 percent of their true values. The remaining coefficients have such a small effect on the trajectory that they cannot be estimated this accurately.

3. Significant coefficient variations with mach number should be modeled and can be estimated by the EKF algorithm.

4. The EKF accurately estimates the rms errors associated with each parameter estimate.

5. Those coefficients which cannot be estimated from the data are identified by the EKF algorithm, and the a priori uncertainties assumed for them remain essentially unchanged.

6. The EKF technique is general and can be adapted to various situations and conditions. It incorporates any a priori knowledge available about the aerodynamic coefficients which might be available from design considerations and wind tunnel tests.

7. The absolute parameter estimation accuracy achievable is sensitive to the particular trajectory motion that occurs, the measurement noise levels, and any modeling errors in the filter design.

SECTION VI

RECOMMENDATIONS

The general EKF technique demonstrated herein can be used as a tool in aerodynamic model development, test evaluations, and ballistic range error-level calibration because of its sensitivity to modeling errors and test conditions. Other possible applications include the reduction of wind tunnel data and the extraction of missile and aircraft aerodynamic coefficients from onboard and external measurements.

The EKF algorithm should be compared with other current data reduction techniques such as the Chapman-Kirk algorithm. Development of an operational algorithm would then be a natural extension of the current work. The algorithm should be evaluated for projectiles other than the 30mm round used in these investigations to assess its performance over a range of aerodynamic bodies. Finally, the expansion of the current model to the asymmetric airframe case should be pursued.

(The reverse of this page is blank.)

APPENDIX A

COMPUTATION OF $F(\hat{\underline{x}}(t),t)$

The propagation of the EKF estimation error covariance matrix, P(t), between measurements requires the computation of the matrix $F(\underline{x}(t),t)$ as indicated in Table 1 and subsection 2.2. This matrix contains the partial derivatives of each filter state derivative with respect to each filter state, evaluated at the current state estimate, $\hat{\underline{x}}(t)$. This appendix gives the equations used to compute this matrix.

PRELIMINARY DEFINITIONS

Table A-1 summarizes the system model upon which the EKF algorithm design is based. The matrix $F(\hat{\underline{x}}(t),t)$ is defined with respect to this model by

$$F(\hat{\underline{x}}(t),t) \equiv \left[\frac{\partial \underline{f}(\underline{x},t)}{\partial \underline{x}}\right]_{\underline{x}=\hat{\underline{x}}} \tag{A-1}$$

Here, the element in the i^{th} row and j^{th} column of F is given by

$$F_{ij}(\hat{\underline{x}},t) = \left[\frac{\partial f_i(\underline{x},t)}{\partial x_j}\right]_{\underline{x}=\hat{\underline{x}}} \tag{A-2}$$

where each function f_i is defined in Table A-1, with its corresponding equation given in Table 6. The expressions given in this appendix for the elements of F are derived by direct differentiation of the appropriate functions. The only assumption made in this derivation is that the air density, ρ, is independent of altitude, z. While not strictly correct, the error induced by this approximation is negligible.

Intermediate Constants

The following variables are defined for convenience and are assumed to be constant for the purposes of computing the required partial derivatives.

$$I_r = I_x/I_y$$
$$r = d/2$$

$$a_m = \rho A/2m$$
$$a_x = \rho Ad/2I_x$$
$$a_y = \rho Ad/2I_y$$

Intermediate Variables and Their Partial Derivatives

The following variables (b_1 through b_5 and k_1 through k_{12}) are functions of the system states. Their definitions are given, followed by their partial derivatives with respect to each state on which they depend.

TABLE A-1. EKF STATE VARIABLE MODEL SUMMARY

INDEX i	ELEMENTS OF STATE VECTOR, x	EQUIVALENT VARIABLE OR COEFFICIENT	VECTOR COMPONENTS		DYNAMIC MODEL, $\dot{\underline{x}} = \underline{f}(\underline{x}, t)$	ELEMENTS OF STATE DERIVATIVE VECTOR, f
1	x_1	x				$f_1 = \dot{x}$
2	x_2	y				$f_2 = \dot{y}$
3	x_3	z				$f_3 = \dot{z}$
4	x_4	u				$f_4 = \dot{u}$
5	x_5	v				$f_5 = \dot{v}$
6	x_6	w	$\underline{v}$		$\dot{\underline{v}} = \underline{g}(\underline{v}, \underline{a})$	$f_6 = \dot{w}$
7	x_7	ϕ			(Given by Table 6)	$f_7 = \dot{\phi}$
8	x_8	θ				$f_8 = \dot{\theta}$
9	x_9	ψ				$f_9 = \dot{\psi}$
10	x_{10}	$\dot{\phi}$				$f_{10} = \ddot{\phi}$
11	x_{11}	$\dot{\theta}$				$f_{11} = \ddot{\theta}$
12	x_{12}	p				$f_{12} = \dot{p}$
13	x_{13}	C_X				$f_{13} = 0$
14	x_{14}	C_{X2}				
15	x_{15}	C_{XV}				
16	x_{16}	$C_{N\alpha}$				
17	x_{17}	$C_{Yp\alpha}$				
18	x_{18}	$C_{m\alpha}$				
19	x_{19}	C_{mq}				
20	x_{20}	$C_{np\alpha}$	$\underline{a}$		$\dot{\underline{a}} = \underline{0}$	
21	x_{21}	C_{lp}				
22	x_{22}	$C_{l\delta}$				
23	x_{23}	$C_{N\alpha 3}$				
24	x_{24}	$C_{Yp\alpha 3}$				
25	x_{25}	$C_{m\alpha 3}$				
26	x_{26}	C_I				
27	x_{27}	C_{mq2}				
28	x_{28}	$C_{np\alpha 3}$				
29	x_{29}	C_{m_V}				$f_{29} = 0$

Variable b_1

$$b_1 = \varepsilon = \sqrt{v^2+w^2}\,/V$$

$$b_{1u} = \partial b_1/\partial u = -u\sqrt{v^2+w^2}\,/V^3$$

$$b_{1v} = \partial b_1/\partial v = \begin{cases} u^2 v/(V^3\sqrt{v^2+w^2}) & \text{if } (v^2+w^2) \neq 0 \\ 1/u & \text{if } (v^2+w^2) = 0 \end{cases}$$

$$b_{1w} = \partial b_1/\partial w = \begin{cases} u^2 w/(V^3\sqrt{v^2+w^2}) & \text{if } (v^2+w^2) \neq 0 \\ 1/u & \text{if } (v^2+w^2) = 0 \end{cases}$$

Variable b_2

$$b_2 = \varepsilon^2 = (v^2+w^2)/V^2$$

$$b_{2u} = \partial b_2/\partial u = 2\varepsilon b_{1u}$$

$$b_{2v} = \partial b_2/\partial v = 2\varepsilon b_{1v}$$

$$b_{2w} = \partial b_2/\partial w = 2\varepsilon b_{1w}$$

Variable b_3

$$b_3 = \bar{C}_{m\alpha} = C_{m\alpha} + C_{m\alpha 3}\varepsilon^2 + C_{m\alpha V}(V_0 - V)$$

$$b_{3u} = \partial b_3/\partial u = C_{m\alpha 3} b_{2u} - uC_{m\alpha V}/V$$

$$b_{3v} = \partial b_3/\partial v = C_{m\alpha 3} b_{2v} - vC_{m\alpha V}/V$$

$$b_{3w} = \partial b_3/\partial w = C_{m\alpha 3} b_{2w} - wC_{m\alpha V}/V$$

Variable b_4

$$b_4 = \bar{C}_{mq} = C_{mq} + C_{mq2}\varepsilon^2$$

$$b_{4u} = \partial b_4/\partial u = C_{mq2} b_{2u}$$

$$b_{4v} = \partial b_4/\partial v = C_{m\alpha 2} b_{2v}$$

$$b_{4w} = \partial b_1/\partial w = C_{mq2} b_{2w}$$

Variable b_5

$$b_5 = \bar{C}_{np\alpha} = C_{np\alpha} + C_{np\alpha 3}\varepsilon^2$$
$$b_{5u} = C_{np\alpha 3} b_{2u}$$
$$b_{5v} = C_{np\alpha 3} b_{2v}$$
$$b_{5w} = C_{np\alpha 3} b_{2w}$$

Variable k_1

$$k_1 = V^2 \bar{C}_X$$
$$k_{1u} = \partial k_1/\partial u = 2u[C_X + (V_0 - 1.5V)C_{XV}]$$
$$k_{1v} = \partial k_1/\partial v = 2v[C_X + C_{X2} + (V_0 - 1.5V)C_{XV}]$$
$$k_{1w} = \partial k_1/\partial w = 2w[C_X + C_{X2} + (V_0 - 1.5V)C_{XV}]$$

Variable k_2

$$k_2 = vV\bar{C}_{N\alpha}$$
$$k_{2u} = \partial k_2/\partial u = uv(C_{N\alpha} - C_{N\alpha 3}\varepsilon^2)/V$$
$$k_{2v} = \partial k_2/\partial v = (v^2+V^2)C_{N\alpha}/V + \left[V^2(3v^2+w^2) - v^2(v^2+w^2)\right] C_{N\alpha 3}/V^3$$
$$k_{2w} = \partial k_2/\partial w = vwC_{N\alpha}/V + vw(V^2+u^2)C_{N\alpha 3}/V^3$$

Variable k_3

$$k_3 = pw\bar{C}_{Yp\alpha}$$
$$k_{3u} = \partial k_3/\partial u = pwb_{2u}C_{Yp\alpha 3}$$
$$k_{3v} = \partial k_3/\partial v = pwb_{2v}C_{Yp\alpha 3}$$

$$k_{3w} = \partial k_3/\partial w = p(\bar{C}_{Yp\alpha} + wb_{2w}C_{Yp\alpha 3})$$
$$k_{3p} = \partial k_3/\partial p = w\bar{C}_{Yp\alpha}$$

Variable k_4

$$k_4 = wV\bar{C}_{N\alpha}$$
$$k_{4u} = \partial k_4/\partial u = uwC_{N\alpha}/V - uw(v^2+w^2)C_{N\alpha 3}/V^3$$
$$k_{4v} = \partial k_4/\partial v = vwC_{N\alpha}/V + vw(V^2+u^2)C_{N\alpha 3}/V^3$$
$$k_{4w} = \partial k_4/\partial w = (w^2+V^2)C_{N\alpha}/V + \left[V^2(3w^2+v^2) - w^2(v^2+w^2)\right]C_{N\alpha 3}/V^3$$

Variable k_5

$$k_5 = pv\bar{C}_{Yp\alpha}$$
$$k_{5u} = \partial k_5/\partial u = pvb_{2u}C_{Yp\alpha 3}$$
$$k_{5v} = \partial k_5/\partial v = p(\bar{C}_{Yp\alpha} + vb_{2v}C_{Yp\alpha 3})$$
$$k_{5w} = \partial k_5/\partial w = pvb_{2w}C_{Yp\alpha 3}$$
$$k_{5p} = \partial k_5/\partial p = v\bar{C}_{Yp\alpha}$$

Variable k_6

$$k_6 = vV\bar{C}_{m\alpha}\sec\theta$$
$$k_{6u} = \partial k_6/\partial u = v\sec\theta\,(V^2b_{3u} + u\bar{C}_{m\alpha})/V$$
$$k_{6v} = \partial k_6/\partial v = \sec\theta\left[vV^2b_{3v} + (v^2+V^2)\bar{C}_{m\alpha}\right]/V$$
$$k_{6w} = \partial k_6/\partial w = v\sec\theta\,(V^2b_{3w} + w\bar{C}_{m\alpha})/V$$
$$k_{6\theta} = \partial k_6/\partial\theta = vV\bar{C}_{m\alpha}\sec\theta\tan\theta$$

Variable k_7

$$k_7 = \dot{\psi} V \bar{C}_{mq}$$

$$k_{7u} = \partial k_7 / \partial u = \dot{\psi}(V^2 b_{4u} + u\bar{C}_{mq})/V$$

$$k_{7v} = \partial k_7 / \partial v = \dot{\psi}(V^2 b_{4v} + v\bar{C}_{mq})/V$$

$$k_{7w} = \partial k_7 / \partial w = \dot{\psi}(V^2 b_{4w} + w\bar{C}_{mq})/V$$

$$k_{7\dot{\psi}} = \partial k_7 / \partial \dot{\psi} = V\bar{C}_{mq}$$

Variable k_8

$$k_8 = pw\bar{C}_{np\alpha} \sec\theta$$

$$k_{8u} = \partial k_8 / \partial u = pwb_{5u} \sec\theta$$

$$k_{8v} = \partial k_8 / \partial v = pwb_{5v} \sec\theta$$

$$k_{8w} = \partial k_8 / \partial w = p(wb_{5w} + \bar{C}_{np\alpha}) \sec\theta$$

$$k_{8\theta} = \partial k_8 / \partial \theta = pw\bar{C}_{np\alpha} \sec\theta \tan\theta$$

$$k_{8p} = \partial k_8 / \partial p = w\bar{C}_{np\alpha} \sec\theta$$

Variable k_9

$$k_9 = wV\bar{C}_{m\alpha}$$

$$k_{9u} = \partial k_9 / \partial u = w(V^2 b_{3u} + u\bar{C}_{m\alpha})/V$$

$$k_{9v} = \partial k_9 / \partial v = w(V^2 b_{3v} + v\bar{C}_{m\alpha})/V$$

$$k_{9w} = \partial k_9 / \partial w = \left[wV^2 b_{3w} + (w^2+V^2)\bar{C}_{m\alpha}\right]/V$$

Variable k_{10}

$$k_{10} = \dot{\theta} V \bar{C}_{mq}$$

$$k_{10u} = \partial k_{10}/\partial u = \dot{\theta}(V^2 b_{4u} + u\bar{C}_{mq})/V$$
$$k_{10v} = \partial k_{10}/\partial v = \dot{\theta}(V^2 b_{4v} + v\bar{C}_{mq})/V$$
$$k_{10w} = \partial k_{10}/\partial w = \dot{\theta}(V^2 b_{4w} + w\bar{C}_{mq})/V$$
$$k_{10\dot{\theta}} = \partial k_{10}/\partial \dot{\theta} = V\bar{C}_{mq}$$

Variable k_{11}

$$k_{11} = pv\bar{C}_{np\alpha}$$
$$k_{11u} = \partial k_{11}/\partial u = pvb_{5u}$$
$$k_{11v} = \partial k_{11}/\partial v = p(vb_{5v}+\bar{C}_{np\alpha})$$
$$k_{11w} = \partial k_{11}/\partial w = pvb_{5w}$$
$$k_{11p} = \partial k_{11}/\partial p = v\bar{C}_{np\alpha}$$

Variable k_{12}

$$k_{12} = pVC_{lp}$$
$$k_{12u} = \partial k_{12}/\partial u = puC_{lp}/V$$
$$k_{12v} = \partial k_{12}/\partial v = pvC_{lp}/V$$
$$k_{12w} = \partial k_{12}/\partial w = pwC_{lp}/V$$
$$k_{12p} = \partial k_{12}/\partial p = VC_{lp}$$

ELEMENTS OF $F(\underline{x},t)$

This subsection gives the expressions for the elements of $F(\underline{x},t)$ in terms of the variables defined in the last section and in subsection 2.2.

Row 1 of $F(\underline{x},t)$

Column, i	$\partial f_1/\partial x_i$
1	0
2	0
3	0
4	$\cos\theta\ \cos\psi$
5	$-\sin\psi$
6	$\sin\theta\ \cos\psi$
7	$-u\ \cos\theta\ \sin\psi - v\ \cos\psi - w\ \sin\theta\ \sin\psi$
8	$-u\ \sin\theta\ \cos\psi + w\ \cos\theta\ \cos\psi$
9	0
⋮	⋮
29	0

Row 2 of $F(\underline{x},t)$

Column, i	$\partial f_2/\partial x_i$
1	0
2	0
3	0
4	$\cos\theta\ \sin\psi$
5	$\cos\psi$
6	$\sin\theta\ \sin\psi$
7	$u\ \cos\theta\ \cos\psi - v\ \sin\psi + w\ \sin\theta\ \cos\psi$
8	$-u\ \sin\theta\ \sin\psi + w\ \cos\theta\ \sin\psi$
9	0
⋮	⋮
29	0

Row 3 of $F(\underline{x},t)$

Column, i	$\partial f_3/\partial x_i$
1	0
2	0
3	0
4	$-\sin\theta$
5	0
6	$\cos\theta$
7	0
8	$-u\cos\theta - w\sin\theta$
9	0
⋮	⋮
29	0

Row 4 of $F(\underline{x},t)$

Column, i	$\partial f_4/\partial x_i$
1	0
2	0
3	0
4	$-a_m k_{1u}$
5	$-a_m k_{1v} + \dot{\psi}\cos\theta$
6	$-a_m k_{1w} - \dot{\theta}$
7	0
8	$g\cos\theta - \dot{\psi}v\sin\theta$
9	0
10	$v\cos\theta$
11	$-w$
12	0
13	$-a_m V^2$

14	$-a_m(v^2+w^2)$
15	$-a_m V^2(V_0-V)$
16	0
⋮	⋮
29	0

Row 5 of $F(\underline{x},t)$

Column, i	$\partial f_5/\partial x_i$
1	0
2	0
3	0
4	$a_m(-k_{2u}+rk_{3u}) - \dot{\psi}\cos\theta$
5	$a_m(-k_{2v}+rk_{3v})$
6	$a_m(-k_{2w}+rk_{3w}) - \dot{\psi}\sin\theta$
7	0
8	$\dot{\psi}(u\sin\theta - w\cos\theta)$
9	0
10	$-u\cos\theta - w\sin\theta$
11	0
12	$a_m rk_{3p}$
13	0
14	0
15	0
16	$-a_m vV$
17	$a_m rpw$
18	0
⋮	⋮
22	0
23	$-a_m vV_c^2$
24	$a_m rpw_c^2$

25	0
⋮	⋮
29	0

Row 6 of $F(\underline{x},t)$

Column, i	$\partial f_6/\partial x_i$
1	0
2	0
3	0
4	$-a_m(k_{4u}+rk_{5u}) + \dot{\theta}$
5	$-a_m(k_{4v}+rk_{5v}) + \dot{\psi}\sin\theta$
6	$-a_m(k_{4w}+rk_{5w})$
7	0
8	$g\sin\theta + \dot{\psi}v\cos\theta$
9	0
10	$v\sin\theta$
11	u
12	$-a_m rk_{5p}$
13	0
14	0
15	0
16	$-a_m wV$
17	$-a_m rpv$
18	0
⋮	⋮
22	0
23	$-a_m wV\varepsilon^2$
24	$-a_m rpv\varepsilon^2$
25	0
⋮	⋮
29	0

Row 7 of $F(\underline{x},t)$

Column, i	$\partial f_7/\partial x_i$
1	0
⋮	⋮
9	0
10	1
11	0
⋮	⋮
29	0

Row 8 of $F(\underline{x},t)$

Column, i	$\partial f_8/\partial x_i$
1	0
⋮	⋮
10	0
11	1
12	0
⋮	⋮
29	0

Row 9 of $F(\underline{x},t)$

Column, i	$\partial f_9/\partial x_i$
1	0
⋮	⋮

⋮	⋮
7	0
8	$\dot{\psi}\cos\theta$
9	0
10	$\sin\theta$
11	0
12	1
13	0
⋮	⋮
29	0

Row 10 of $F(\underline{x},t)$

Column, i	$\partial f_{10}/\partial x_i$
1	0
2	0
3	0
4	$a_y\left[-k_{6u}+r(k_{7u}+k_{8u})\right]$
5	$a_y\left[-k_{6v}+r(k_{7v}+k_{8v})\right]$
6	$a_y\left[-k_{6w}+r(k_{7w}+k_{8w})\right]$
7	0
8	$a_y(-k_{6\theta}+rk_{8\theta}) + 2\dot{\theta}\dot{\psi}\sec^2\theta + C_I I_r \dot{\theta} p \sec\theta \tan\theta$
9	0
10	$a_y r k_{7\dot{\psi}} + 2\dot{\theta}\tan\theta$
11	$2\dot{\psi}\tan\theta + C_I I_r p \sec\theta$
12	$a_y r k_{8p} + C_I I_r \dot{\theta}\sec\theta$
13	0
⋮	⋮
17	0
18	$-a_y v V \sec\theta$
19	$a_y r \dot{\psi} V$

20	$a_y rpw \sec\theta$
21	0
⋮	⋮
24	0
25	$-a_y vV\varepsilon^2 \sec\theta$
26	$I_r \dot{\theta} p \sec\theta$
27	$a_y r\dot{\psi} V\varepsilon^2$
28	$a_y rpw\varepsilon^2 \sec\theta$
29	$-a_y vV(V_0-V)\sec\theta$

Row 11 of $F(\underline{x},t)$

Column, i	$\partial f_{11}/\partial x_i$
1	0
2	0
3	0
4	$a_y\left[k_{9u}+r(k_{10u}+k_{11u})\right]$
5	$a_y\left[k_{9v}+r(k_{10v}+k_{11v})\right]$
6	$a_y\left[k_{9w}+r(k_{10w}+k_{11w})\right]$
7	0
8	$C_I I_r \dot{\psi} p \sin\theta - \dot{\psi}^2(\cos^2\theta-\sin^2\theta)$
9	0
10	$-C_I I_r p \cos\theta - 2\dot{\psi} \cos\theta \sin\theta$
11	$a_y rk_{10}\dot{\theta}$
12	$a_y rk_{11p} - C_I I_r \dot{\psi} \cos\theta$
13	0
⋮	⋮
17	0
18	$a_y wV$
19	$a_y r\dot{\theta} V$

20	$a_y rpv$
21	0
⋮	⋮
24	0
25	$a_y wV\varepsilon^2$
26	$-I_r \dot{\psi} p \cos\theta$
27	$a_y r\dot{\theta} V\varepsilon^2$
28	$a_y rpv\varepsilon^2$
29	$a_y wV(V_0-V)$

Row 12 of $F(\underline{x},t)$

Column, i	$\partial f_{12}/\partial x_i$
1	0
2	0
3	0
4	$a_x(rk_{12u}+2uC_{l\delta})$
5	$a_x(rk_{12v}+2vC_{l\delta})$
6	$a_x(rk_{12w}+2wC_{l\delta})$
7	0
⋮	⋮
11	0
12	$a_x rk_{12p}$
13	0
⋮	⋮
20	0
21	$a_x rpV$
22	$a_x V^2$
23	0
⋮	⋮
29	0

Rows 13 through 29 of $F(\underline{x},t)$

Since $f_i(\underline{x},t) = 0$ for $i = 13,\ldots,29$, then all elements in rows 13 through 29 are zero.

REFERENCES

1. Gelb, A., Ed., Applied Optimal Estimation, MIT Press, Cambridge, Massachusetts, 1974.

2. Jazwinski, A.H., Stochastic Processes and Filtering Theory, Academic Press, New York, 1970.

3. Sage, A.P., Optimum Systems Control, Prentice-Hall, Inc., Englewood Cliffs, New Jersey, 1968.

4. Nahi, N.E., Estimation Theory and Applications, John Wiley and Sons, Inc., New York, 1969.

5. Kalman, R.E., "A New Approach to Linear Filtering and Prediction Theory," Transactions of the ASME, Journal of Basic Engineering, March 1960, pp 35-45.

6. Daniel, D.C., "An Analysis of Methods for Extracting Aerodynamic Coefficients from Test Data," AFATL-TR-73-32, Air Force Armament Laboratory, February 1973.

7. Whyte, R.H. and Hathaway, W.H., "Aeroballistic Range Data Reduction Technique Utilizing Numerical Integration," AFATL-TR-74-41, Air Force Armament Laboratory, February 1974.

8. Price, C.F. and Koenigsberg, W.D., "Adaptive Control with Explicit Parameter Identification for Tactical Missiles," TR-170-3, The Analytic Sciences Corp., 1 December 1971, AD735488.

(The reverse of this page is blank.)

INITIAL DISTRIBUTION

HQ USAF/RDQRM	1	AF SPEC COMM CNTR/SUR	3
HQ USAF/SAMI	1	DAMA-WSA	1
HQ USAF/XOXFCM	1	SARPA-ER-S-A	1
AFSC/TGFG	1	US Atomic Energy Commission/ Hqs Library	1
AFSC/SDZA	1		
HQ AFSC/DLCAW	1	AEDC/ARO/DLCS	1
AFWL/DO/AMIC	1	AMXSY-DS	1
HQ 4950 Test Wing/TZHM	1	AMCRD-WM	1
AFIT/LD	1	Nav Wpns Eval Fac/Code WT	1
ASD/ENFEA	1	Office of the Chief of Nav Opns/ (OP-982E)	1
ASD/ENAE	1		
AFFDL/FES	1	Naval Research Lab/Code 2627	1
TAC/DRA	1	HQ PACAF/LGWSE	4
SAC/LGWC	1	USAFTAWC/TE	1
HQ SAC(NRI/STINFO LIB)	1	TAWC/TRADOCLO	1
WRAMA/MMEBL	1	AFATL/DL	1
CIA, CRE/ADD/PUBS	2	AFATL/DLY	1
AFWL/LR	1	AFATL/DLOU	1
AUL (AUL-LSE-70-239)	1	AFATL/DLOSL	9
SARRI-LW-A	1	AFATL/DLYV	1
AMXSY-DD	1	AFATL/DLDL	20
AMXSY-A	1	AFATL/DLDA	1
DRXBR-TE	1	AFATL/DLDE	1
Frankford Arsenal/Lib-K2400	1	AFATL/DLDT	1
SARPA-TS	1	AFATL/DLDG	1
Dahlgren Laboratory	1	AFIS/INTA	1
White Oak Laboratory	2	NAV SEA SYS COMD/Code SEA-0332	1
NAV ORD STN/Tech Lib	1	NAV SEA SYS COMD/Code SEA-992E	1
NAV WEAPONS STN/20323	1	NAV ORD LAB	2
NAV UNDERWATER SYS CTR/Code 54	1	Naval Weapons Center/Code 32602	1
USN WEA CTR/Code 233	2	Naval Weapons Center/Code 3163	1
NAV WPNS CTR/Code 31	1	Ogden ALC/MMWRA	2
AF WPNS LAB/Tech Lib	1	AFLC/MMWMC	1
NAV AIR SYS COMD/Code 5323	1	ASD/ENESS	1
Office Naval Research/Code 473	1	AFATL/DLJ	2
Univ of California/Lawrence Rad Lab	1	AFATL/DLA	1
The John Hopkins University/ Applied Physics Lab	1	ADTC/SDC	1
		Redstone Sci Info Cntr	1
Battelle Memorial Inst/Reports Lib	1	General Electric Co./Armament Systems Dept	10
Inst for Defense Analysis/Class Lib	1		
Sandia Laboratories	2	NASA/Acquisitions Br	1
The RAND Corporation	1		
DDC/TC	12		
USAFTFWC/TA	1		
SARWV-RDT-L	1		
NAV WPNS CTR/Code 3123	1		
Ogden ALC/MMWM	2		

(The reverse of this page is blank)